

Estimates of New and Total Productivity in Central Long Island Sound from In Situ Measurements of Nitrate and Dissolved Oxygen

James R. Collins · Peter A. Raymond ·
W. Frank Bohlen · Mary M. Howard-Strobel

Received: 8 March 2012 / Revised: 12 September 2012 / Accepted: 18 September 2012 / Published online: 20 October 2012
© Coastal and Estuarine Research Federation 2012

Abstract Biogeochemical cycles in estuaries are regulated by a diverse set of physical and biological variables that operate over a variety of time scales. Using in situ optical sensors, we conducted a high-frequency time-series study of several biogeochemical parameters at a mooring in central Long Island Sound from May to August 2010. During this period, we documented well-defined diel cycles in nitrate concentration that were correlated to dissolved oxygen, wind stress, tidal mixing, and irradiance. By filtering the data to separate the nitrate time series into various signal components, we estimated the amount of variation that could be ascribed to each process. Primary production and surface wind stress explained 59 and 19 %, respectively, of the variation in nitrate concentrations. Less frequent physical forcings, including large-magnitude wind events and spring tides, served to decouple the relationship between oxygen, nitrate, and sunlight on about one quarter of study days. Daytime nitrate minima and dissolved oxygen maxima occurred nearly simultaneously on the majority (>80 %)

of days during the study period; both were strongly correlated with the daily peak in irradiance. Nighttime nitrate maxima reflected a pattern in which surface-layer stocks were depleted each afternoon and recharged the following night. Changes in nitrate concentrations were used to generate daily estimates of new primary production ($182 \pm 37 \text{ mgCm}^{-2}\text{day}^{-1}$) and the f ratio (0.25), i.e., the ratio of production based on nitrate to total production. These estimates, the first of their kind in Long Island Sound, were compared to values of community respiration, primary productivity, and net ecosystem metabolism, which were derived from in situ measurements of oxygen concentration. Daily averages of the three metabolic parameters were $1,660 \pm 431$, $2,080 \pm 419$, and $429 \pm 203 \text{ mgCm}^{-2}\text{day}^{-1}$, respectively. While the system remained weakly autotrophic over the duration of the study period, we observed very large day-to-day differences in the f ratio and in the various metabolic parameters.

J. R. Collins · P. A. Raymond
School of Forestry & Environmental Studies, Yale University,
New Haven, CT 06511, USA

J. R. Collins (✉)
MIT/WHOI Joint Program in Oceanography/Applied Ocean
Science and Engineering, Department of Marine Chemistry &
Geochemistry,
Woods Hole, MA 02543, USA
e-mail: jrcollins@whoi.edu

W. F. Bohlen · M. M. Howard-Strobel
Department of Marine Sciences, University of Connecticut,
Groton, CT 06340, USA

Keywords Long Island Sound · Nitrate · Nitrogen · New production · In situ measurements · Eutrophication · Dissolved oxygen · Net ecosystem metabolism · Wind forcing · Wind stress · f ratio

Introduction

Nearly 100,500 t of nitrogen is exported annually to Long Island Sound (LIS), a large estuary in the densely populated and highly developed northeastern USA (NYSDEC and CTDEP 2000). Most of this nitrogen has an anthropogenic origin: By the most recent estimate, roughly 66 % of the LIS

nitrogen load comes from human activities such as wastewater transport and treatment, agriculture (fertilizers and animal wastes), and the burning of fossil fuels. Nearly a quarter of the anthropogenic nitrogen load is injected by tributary rivers and streams or deposited directly from the atmosphere onto the water surface. The majority of the anthropogenic load (58.7 %) comes from point sources, including wastewater treatment plants and combined sewer overflows, that feed directly into the Sound (NYSDEC and CTDEP 2000).

The large inputs of nitrogen to LIS have led to eutrophication, particularly in the western part of the basin. Eutrophication has profound and adverse effects on the health of estuaries worldwide (Breitburg et al. 2009; Diaz and Rosenberg 2008; Ryther and Dunstan 1971; Zhang et al. 2010). In LIS specifically, eutrophication is responsible for recurring patterns of seasonal hypoxia (Anderson and Taylor 2001; O'Donnell et al. 2008; Welsh and Eller 1991), blooms of harmful “brown tide” algae and neurotoxin-producing cyanobacteria (Bushaw-Newton and Sellner 1999), and the alteration of basic ecosystem trophic structures (Capriulo et al. 2002).

Combined measurements of primary production, respiration, and net ecosystem metabolism (NEM) have been elegantly applied to assess the health and trophic status of a wide variety of coastal marine ecosystems and estuaries for at least the last half century (Caffrey 2003; Howarth et al. 1992; Kemp and Boynton 1980; Odum 1956; Smith 2007; Swaney et al. 1999). There continues to be considerable attention to quantifying the relationship between nitrogen loading and primary production in many estuaries (Caffrey 2004; D'Avanzo et al. 1996; Nixon 1992). By comparing rates of primary production and nitrogen loading as we do here, one may obtain an index of eutrophication that can be used to make comparisons across ecosystems and through time (Smith 2007).

Most of Long Island Sound's nitrogen load is in the forms of nitrate (NO_3^-) and ammonium (NH_4^+) (Anderson and Taylor 2001). In Long Island Sound as in other eutrophic embayments, nitrate is of particular concern because it is the form most readily assimilated by primary producers, entering the surface layer from either below the pycnocline or from allochthonous inputs such as freshwater runoff and sewage. Once allochthonous nutrients are delivered to the surface layer, they become the basis for what Dugdale and Goering (1967) termed “new” production. This new production, much of it often based on anthropogenic sources, is of particular concern in temperate coastal ecosystems, where it frequently accounts for a very large share of total productivity (Carpenter and Dunham 1985) and net oxygen and metabolism changes.

Various biological and physical processes act over multiple timescales to determine the delivery of nitrate to the surface

layer and its subsequent uptake by phytoplankton (Collos 1998; Garside 1985; Johnson 2010; Probyn et al. 1996). The apportioning of variation among these various processes, particularly those that define nitrate concentrations on hourly and sub-hourly timescales, demands further research in the coastal ocean. Prior to the development of in situ spectrophotometric methods that measure concentrations at very high sampling intervals (Johnson 2010; Johnson et al. 2006), studies examining the impact of wind forcing and other controls in situ were largely restricted to theory and to anecdotal evidence obtained through fortuitous circumstances at sea (Andersen and Prieur 2000; Eppley and Renger 1988). Bearing in mind the relative importance of anthropogenic nitrate inputs to the overall state of eutrophication in Long Island Sound, we utilize high-frequency measurements to couple nitrate-based estimates of new production with estimates of gross primary productivity and ecosystem metabolism based on free-water dissolved oxygen (DO) concentrations.

Methods

Study Site

Automated, high-resolution in situ observations of nitrate, dissolved oxygen, water temperature, conductivity, chlorophyll fluorescence, turbidity, and incident photosynthetically active radiation (PAR) were made at 15-min intervals from the Central Sound Buoy, a mooring in central Long Island Sound, from May to August 2010. The buoy (position 41°8.25'N, 072°39.30'W, approximately 14.3 km south of Guilford, CT, USA) is one of four permanent moorings that, together with a number of fixed stations, comprise the University of Connecticut's LISICOS monitoring network (formerly MYSound; Tedesco et al. 2003). As such, the buoy has a suite of calibrated meteorological instruments that provided us with additional high-frequency observations of wind velocity, wave height, air temperature, and barometric pressure. The site lies roughly along the major east–west axis of the estuary and is coincident with Connecticut Department of Energy and Environmental Protection (CTDEEP; formerly CTDEP) station I2, one of 17 designated stations at which the agency has made monthly observations of water quality since 1994 (Fig. 1). Depth at the Central Sound Buoy station is 27 m, which is slightly deeper than the LIS average of approximately 20 m (Bowman 1977).

The site is nearly equidistant from the Connecticut coastline (14 km) and the north shore of Long Island (17 km). The site's distance from land, considerable water depth, and immediate bathymetry distinguish it from both the coastal ocean at the eastern mouth of the Sound and from the shallower, more heavily eutrophied waters of the Sound's western reaches. While the central Sound does not experience the recurring low oxygen conditions typical at the

westernmost sites, it is still somewhat sheltered from the full energy of the Atlantic Ocean. Reduced tidal forcing and the considerable lee provided by Long Island to the site's south mean it does not experience the degree of water-mass advection that is observed at more easterly sites.

Additional data reported in this study were collected by CTDEEP at monitoring stations elsewhere in the Sound (Fig. 1). Rainfall observations are reported for KHVN (at Tweed-New Haven Airport), the closest weather station maintained by the US National Weather Service; the airport is 24.6 km northwest of the study site. Collection of discrete samples and instrument maintenance at the site were performed aboard R/V *Catch the Joy*, a 23-ft Parker owned and operated for research on Long Island Sound by the Yale School of Forestry & Environmental Studies. The vessel was moored at the Yale-Peabody Marine Station in Guilford, CT, USA.

Automated Observations

Data from in situ instrumentation were recorded at 15-min intervals by a Campbell Scientific data logger onboard the mooring; these data were transmitted to shore via cellular telemetry, where they were downloaded to a server at the University of Connecticut.

Nitrate

Nitrate was estimated at ~2 m depth using data from a Submersible Ultraviolet Nitrate Analyzer (SUNA), a commercially available, 256-channel in situ ultraviolet spectrophotometer (Satlantic Inc., Halifax, NS, Canada). The SUNA is an "off the shelf" version of the In Situ Ultraviolet Spectrophotometer developed at the Monterey Bay Aquarium Research Institute (Johnson and Coletti 2002; Johnson et al. 2006). The SUNA uses factory-installed software to determine nitrate concentrations in real time from an absorbance spectrum between 217.5 and 240 nm; these onboard estimates were useful for remote monitoring of the instrument's fouling condition during peak periods of productivity, but proved not to be as accurate at estimating nitrate as the *post hoc* calculations we performed using the raw spectral data. The onboard algorithm often overestimated nitrate concentrations by 2–3 μM in the moderately brackish (26–28 psu) waters at the study site.

Nitrate concentrations reported in this study were instead calculated using the method described in Sakamoto et al. (2009), in which simultaneously collected temperature and conductivity data are applied to correct for absorbance of the bromide ion. Bromide absorbs light at many of the same wavelengths as nitrate. CTD data are used to predict bromide

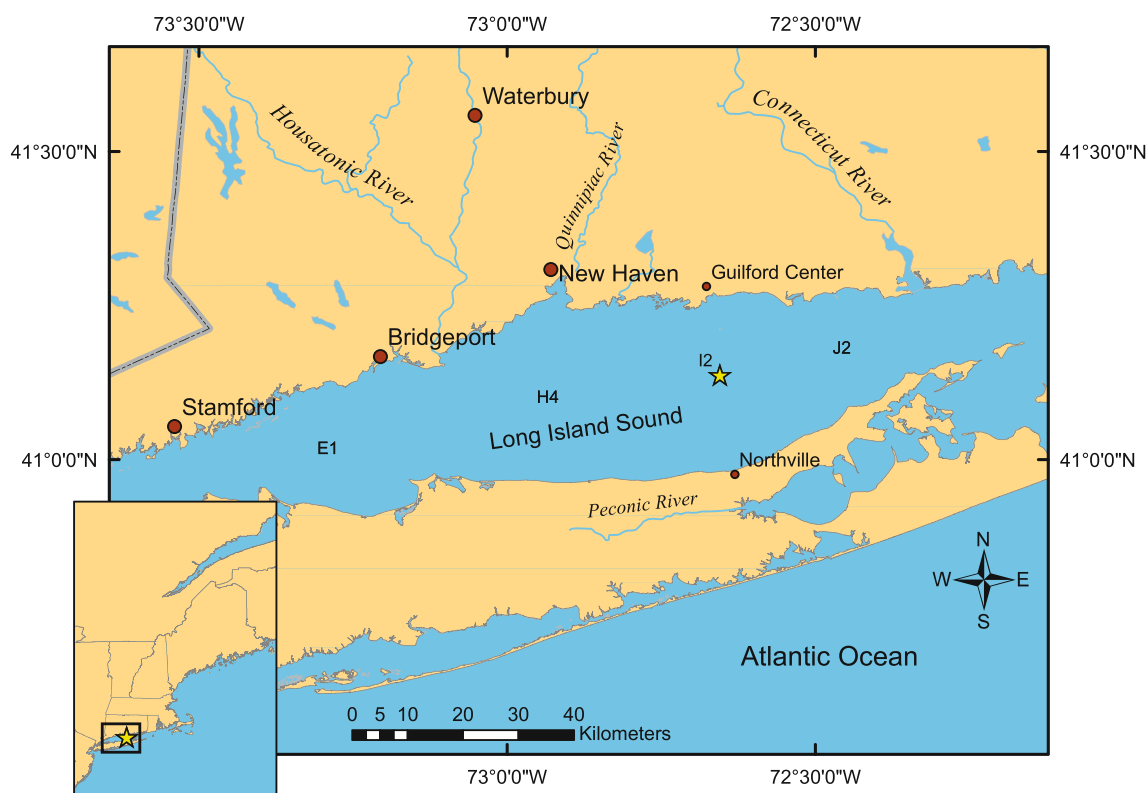


Fig. 1 Mooring location (★; 41°8.25'N, 072°39.30'W; 27 m depth) in central Long Island Sound and selected CTDEEP water quality monitoring stations (E1, H4, I2, and J2) referenced in this study. Station I2 is coincident with the study site

concentration using the known bromide-to-chlorinity ratio; the instantaneous UV spectrum due to bromide is then computed from temperature-corrected molar absorptivity (Sakamoto et al. 2009). This spectrum is subtracted from the observed spectrum, which, when combined with a baseline absorbance, yields the concentration of nitrate. Calibrations were performed in the laboratory at a variety of temperatures and salinities that bracketed the range of temperatures and salinities observed during the study period.

SUNA Calibration and Validation

Final, temperature-corrected, salinity-subtracted nitrate concentrations were validated against discrete samples collected in triplicate at the study site. Filtration to $0.7 \mu\text{m}$ with a combusted Whatman GF/F filter was performed in the field using acid-washed tubing and filter holder directly into acid-washed high-density polyethylene bottles; samples were immediately frozen. Determination of nitrate was performed by automated colorimetric titration at two independent laboratories. Samples were analyzed by segmented flow analysis (Astoria-Pacific Inc., Clackamas, OR, USA; method detection limit $0.007 \mu\text{M}$) at the Yale Analytical Laboratory and by flow injection analysis (SmartChem discrete analyzer, Unity Scientific, LLC, Brookfield, CT, USA; method detection limit

$0.005 \mu\text{M}$) at the University of New Hampshire Water Quality Analysis Lab. Orthophosphate was also determined by segmented flow analysis at the Yale facility.

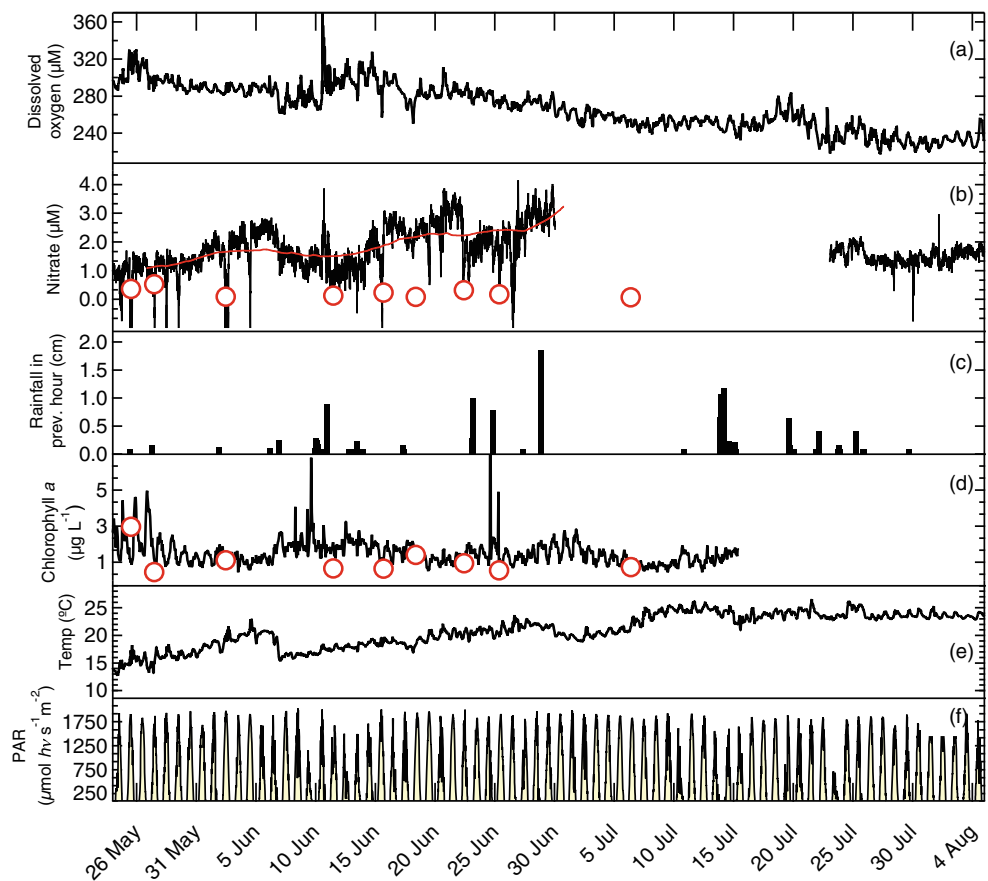
Biofouling

Biofouling of the instrument was monitored by both visual inspections during regular cruises to the site and by examining drift in the baseline of the UV absorption spectrum in the real-time data. A perforated copper guard was installed over the optical chamber window to inhibit marine growth, and preventative manual cleaning of the optic was performed during each site visit with a soft cloth and 10 % HCl solution. However, approximately 1 month of data from the SUNA was discarded due to evidence of fouling, which occurred during a period from 30 June to 25 July when visits could not be made to the site (Fig. 2).

Other Automated Measurements

DO, water temperature, and conductivity were measured using a YSI 6600 series submersible sonde (YSI Inc., Yellow Springs, OH, USA). The DO, temperature, and conductivity sensors onboard the mooring were calibrated according to manufacturer specifications and LISICOS (formerly

Fig. 2 Time series observations over the course of the study period at the study site in central Long Island Sound: **a** dissolved oxygen, **b** nitrate, **c** rainfall for the previous hour at Tweed-New Haven Airport, **d** chlorophyll *a*, **e** sea surface temperature, and **f** photosynthetically active radiation. The open (red) circles are concentrations of nitrate and chlorophyll *a* in discrete samples. The red trace in **b** is a low-pass Fourier transform, showing the long-term trend in the nitrate data set. A segment of the nitrate data is omitted from the period during which biofouling was discovered on the SUNA



MYSound) operating procedures (Tedesco et al. 2003) prior to the study period on 28 April 2010, once during the study period, and then upon completion of the study period in September 2010. Chlorophyll fluorescence was measured at 1 m depth using a YSI 6025 series chlorophyll fluorometer. Turbidity in units of NTU was measured at 2 m depth using a Campbell Scientific OBS-3+ turbidity sensor (Campbell Scientific Inc., Logan, UT, USA). Calibration was performed according to manufacturer specifications using a series of AmcoClear SDVB nephelometric turbidity standards. The concentration of total suspended solids (TSS) was determined from turbidity using a regression (not shown) based on data from a nearby site in Long Island Sound (OSI 2009).

Over the course of the study period, drift was noted in two of these instruments. First, after heavy biofouling was discovered, we discarded segments of the conductivity data from 4 to 21 of July and 6 to 10 of August. Given the small and predictable linear increase in salinity that historically occurs over the course of the summer months in the central Sound (Riley 1956), we interpolated the missing values from historical averages and CTDEEP data (Matthew Lyman, CTDEEP, unpublished data).

A smaller segment of the turbidity data (from 7 June to 14 June) was discarded as a result of similar fouling. Since turbidity remained extremely low throughout the study period, consistent with historical observations for this region of the Sound (Matthew Lyman, CTDEEP, unpublished data), we averaged the values over 2 days on either side of the gap and then interpolated using that figure.

Irradiance was measured at approximately 3 m above the sea surface using a LI-COR LI190SB photosynthetic photon flux sensor (LI-COR Biosciences Inc., Lincoln, NE, USA). A TRIAXYS Directional wave sensor (AXYS Technologies Inc., Sidney, BC, Canada) provided real-time data on wave height, direction, and period. Anemometer height was 3.5 m above the sea surface.

Collection of Discrete Samples

Chlorophyll a

Volumetric filtrations of seawater collected at the study site were performed for chlorophyll *a* at the Yale-Peabody Marine Station following each site cruise. Triplicate 25-mm Whatman GF/F filters (0.7 μm pore size) were frozen immediately pending analysis; determination of chlorophyll was performed in the laboratory according to US Environmental Protection Agency method 445.0 (Arar and Collins 1997) on a Turner Designs TD-700 fluorometer (Turner Designs, Sunnyvale, CA, USA). A calibration curve based on these values (not shown) was then used to obtain a high-resolution, pheophytin-corrected chlorophyll *a* time series (Figs. 2d and 4c) from the in situ chlorophyll fluorescence data.

DOC and TDN

Triplicate samples were collected for analysis of dissolved organic carbon (DOC) and total dissolved nitrogen (TDN) in acid-washed polycarbonate bottles. Filtration was performed in the field directly into sample bottles using a Cole-Parmer peristaltic field pump (Cole-Parmer Inc., Vernon Hills, IL, USA), combusted Whatman GF/F filter (0.7 μm pore size), and acid-washed tubing. Samples were immediately frozen. Upon thawing, quantification of DOC and TDN was performed immediately by high-temperature catalytic oxidation on a TOC-V_{CSH} total organic carbon/total nitrogen analyzer (Shimadzu Inc., Columbia, MD, USA; detection limit of 4 $\mu\text{g L}^{-1}$ for TOC and 0.1 mg L^{-1} for TDN).

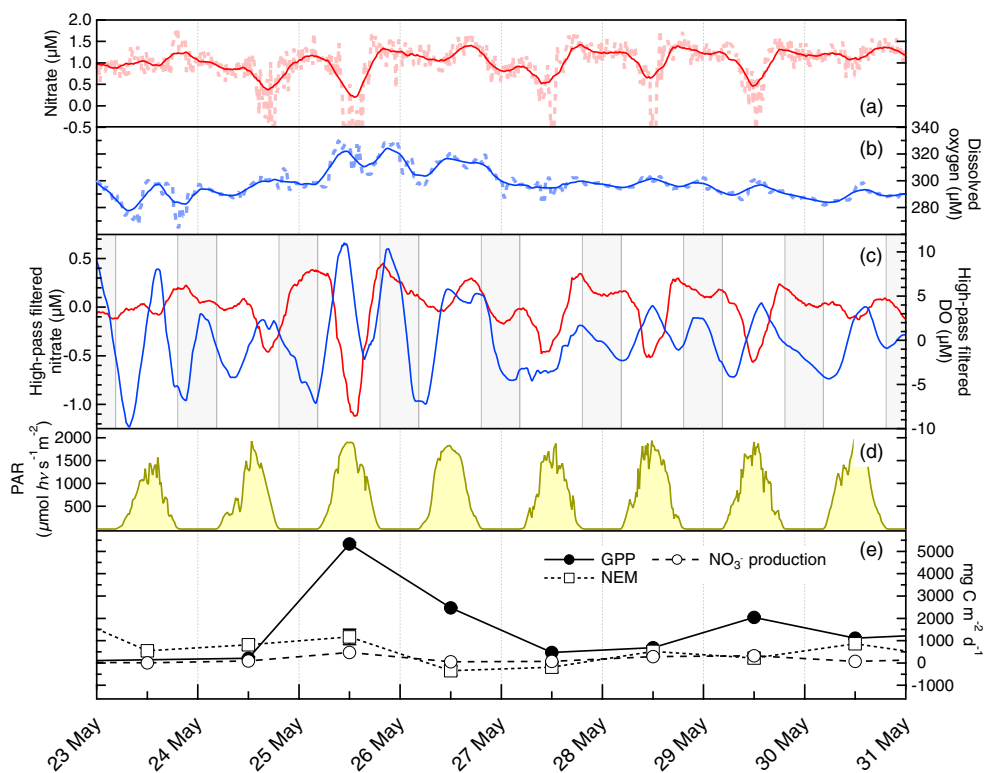
High-Pass and Low-Pass Signal Processing

To isolate diel, photosynthetically driven cycles of nitrate and DO concentrations from longer-term trends in the same variables, we applied fast Fourier transforms using the “TSA” (Chan 2008) and “mFilter” (Balcilar 2009) libraries for R (version 2.10.1), a statistical computing package, according to the methods described in Cryer and Chan (2008). We applied transforms only to the nitrate and dissolved oxygen data, yielding two complementary datasets that we used for different purposes. First, we created a nitrate-dissolved oxygen dataset that excluded all cycles with periods >25 h (Fig. 3 c); from this first dataset, we also excluded sources of very high-frequency variation (i.e., signals with periods <2.5 h). This second step eliminated any stochastic noise in the data that would have interfered with the amplitude analysis described below. We then produced a second, complementary dataset using only a low-pass filter; this dataset included only long-term trend components of the nitrate and dissolved oxygen signals. We used the first dataset to estimate nitrate-based primary production (see Section 2.5.2 below) and to examine correlations at sub-daily timescales between dissolved oxygen, nitrate concentration, photosynthetically active radiation, and other variables. We used the second dataset to examine long-term trends in dissolved oxygen and nitrate concentration. Time-series analysis techniques have been applied successfully in several other recent studies to separate different signal components in high-resolution biogeochemical datasets, including those based on in situ spectrophotometric data (Johnson 2010; Johnson et al. 2006).

Data Analysis: Determination of Community Metabolic Parameters

We report community metabolic parameters as depth-integrated values for the euphotic zone at the study site. The vast majority of values reported in the literature from

Fig. 3 Observations of **a** nitrate (solid line), **b** dissolved oxygen (dashed line), **c** high-pass filtered nitrate and dissolved oxygen, and **d** photosynthetically active radiation during a representative 9 day period (23–31 May 2010) at the mooring in central Long Island Sound. A high-pass Fourier transformation of the nitrate and DO datasets (**c**) emphasizes the inverse daytime relationship between nitrate assimilation and DO production, which we exploited to estimate rates of ecosystem metabolism and new production in **e**. The diel oscillations in DO, nitrate, and PAR evident in **a–d** plots are coupled through the central processes of photosynthesis and respiration



similar studies are in areal units, i.e., integrated over the depth of the euphotic zone. While there are some disadvantages to the use of depth-integrated estimates in assessments of coastal eutrophication (see, e.g., Smith 2007), we concluded that our results would be most useful to others in this form.

Depth of Euphotic Zone (Z_{eu})

The depth of the euphotic zone was estimated from our automated, in situ observations of PAR, chlorophyll *a* fluorescence, conductivity, and TSS, using a parameterization developed for a large temperate estuary (Xu et al. 2005):

$$K_d(PAR) = 1.17 + 0.024 \times [chl-a] + 0.006 \times [TSS] - 0.0225 \times S \tag{1}$$

and the relationship (Kirk 2011)

$$Z_{eu} = \frac{4.6}{K_d} \tag{2}$$

where K_d (PAR) is the light attenuation for photosynthetically active radiation, [chl-*a*] is the concentration of chlorophyll *a* in micrograms per liter, [TSS] is the concentration of total suspended solids in milligrams per liter, *S* is the salinity, and Z_{eu} is the depth of the euphotic zone. This method uses the sum of three parameters to approximate the individual contributions of each constituent to the attenuation and scattering of each wavelength of photosynthetically active light; it thus involves considerable assumptions about

the inherent optical properties of the water at our study site (Kirk 1984; Kirk 2003). Z_{eu} was estimated from the data at 15-min intervals; the values were then averaged over the course of each 24-h day.

While this parameterization was developed for the lower reaches of the Chesapeake Bay, it functioned as a reasonable, if not ideal, means of estimating euphotic zone depth in Long Island Sound during our study period. To validate the applicability of the model, we compared the depth estimates to both Secchi disk measurements we made at the site during each of our sampling cruises ($n=10$) and to PAR profiles from monthly CTDEEP CTD casts at Station I2 ($n=3$). While these two independent measures generally confirmed the applicability of the model to conditions at our study site, the model underestimated Z_{eu} by 2 m relative to the May CTD profile (data not shown).

New Production Based on Nitrate

To determine the quantity of new biomass produced through uptake of allochthonous nitrate over the course of each daylight period, we calculated changes in daily nitrate concentrations ($-\Delta NO_3^-$; micromoles of NO_3^- per liter per hour) for each daylight hour using the high-pass-filtered nitrate dataset. The daily sum of these changes represents the rate of new production (in $-\mu mol NO_3^- L^{-1} day^{-1}$).

Volumetric estimates of new production were normalized to a 12-h day and then converted to estimates in units of

milligrams of C per cubic meter per day as described in Johnson et al. (2006) by invoking the ratio identified by Redfield (1934), i.e., $-\Delta\text{NO}_3$ ($\mu\text{molNL}^{-1}\text{day}^{-1}$) $\times 6.6 \mu\text{mol C}/\mu\text{molN} \times 12 \mu\text{gC}/\mu\text{molC}$. The volumetric production rate was then integrated over the depth of the euphotic zone. Rates of new production were not calculated for the period of study during which fouling of the SUNA occurred.

Respiration and Primary Production

We estimated rates of respiration and primary production from observed changes in dissolved oxygen concentration in the bulk free water mass at the study site. Variations of this method have been successfully applied to estimate ecosystem metabolism in a number of other estuaries (Caffrey 2003, 2004; D'Avanzo et al. 1996; Johnson et al. 1981) and in offshore systems (DeGrandpre et al. 1997; Johnson et al. 1981; Johnson 2010). During daylight hours, two processes occur. Oxygen is evolved as an end-product of photosynthesis in proportion to available light, nutrients, and other factors; and some amount of oxygen is consumed through respiration, generally as a terminal electron acceptor. In the absence of light, only respiration occurs. Staehr et al. (2012) provide a useful synthesis of the diel oxygen flux method as it currently used in several ecosystem types.

We estimated rates of ecosystem metabolism in grams of O_2 per cubic meter per hour from observed changes in dissolved oxygen over each 1-h time interval during the study. For these estimates, we used unfiltered dissolved oxygen data (i.e., data without any signal processing). First, we estimated the mean DO concentration at the top of each hour by averaging the 15-min observations over the previous time interval. We then calculated a depth-integrated rate of change in units of grams of O_2 per square meter per hour according to the formula (after Caffrey 2004)

$$\text{Oxygen flux} = (\text{DO}_{t2} - \text{DO}_{t1}) \times Z_{eu} + F \quad (3)$$

where DO_{t1} and DO_{t2} are the concentrations at the beginning and end of each hour, Z_{eu} is the depth of the euphotic zone, and F is the air–sea flux over the given time period. Because we did not have a bottom-layer oxygen sensor or benthic flux chamber, our method does not directly capture any contribution from the benthos. While our study focuses exclusively on water-column processes and we make no claims to account for the benthos, we do assume based on the site's 27 m water depth that our free water measurements in the pelagic zone provide a reasonable approximation for overall ecosystem metabolism. In estuaries, the relative contribution of benthic respiration to total ecosystem metabolism generally decreases with depth when the depth exceeds a threshold of approximately 10 m (Hopkinson and Smith 2005).

To obtain daily rates of community respiration, R_c , we first calculated a mean hourly rate of respiration, R_h , by adding the estimated hourly fluxes over each nighttime period and dividing by the number of hours of darkness. We then extrapolated this rate to a 24-h day, assuming that respiration was not significantly different during the daytime, to obtain a rate in grams of O_2 per square meter per day. Because respiration is conventionally a positive quantity, we multiplied this value by -1 .

We then calculated a rate of daytime net community production, NCP_d , by adding the oxygen fluxes over each daylight hour. We estimated daily rates of gross primary production, GPP, and net ecosystem metabolism, NEM, according to the formulae

$$\text{GPP} = \text{NCP}_d + R_c \quad (4)$$

and

$$\text{NEM} = \text{GPP} - R_c \quad (5)$$

We converted daily rates from units of grams of O_2 per square meter per day to milligrams of C per square meter per day assuming a respiratory quotient (moles of O_2 /moles of C) of 1.0 and, based on previous work specific to Long Island Sound, a photosynthetic quotient of 1.2, i.e., $1 \text{ g O}_2 \times 1 \text{ mol O}_2/32 \text{ g O}_2 \times 1 \text{ mol C}/1.2 \text{ mol O}_2 \times 12 \text{ g C}/1 \text{ mol C} \times 1,000 \text{ mgC}/1 \text{ gC}$ (Goebel and Kremer 2007).

Tidal Advection

As in most studies employing fixed moorings, tidal advection in Long Island Sound induces the movement of distinct water masses past our study site with different physical and chemical properties; these water masses may, for example, have different concentrations of dissolved oxygen and nitrate. In considering a time series such as the one presented here, one must therefore employ some method to correct for or exclude this additional source of variation. Tidal circulation in LIS is dominated by the lunar semidiurnal, or M_2 , component, which has an approximate period of 12.4 h (Bennett et al. 2010; Kenefick 1985). By basing our estimates on hourly flux measurements (and not, as we might have done, on a single measurement of $\Delta[\text{O}_2]$ or $\Delta[\text{NO}_3^-]$ over the course of the 24-h production day), we attempt to exclude any signals with a period >1 h, including the 12.4-h tidal component.

While we are confident our method excludes much of this unwanted variation, our estimates likely still reflect some artifact of tidal advection. By calculating the maximum possible tidal excursion of a given water mass in any direction from the study site, we can roughly estimate the surface area that would be integrated by our method if we were unsuccessful at excluding unwanted variation. This figure is

a basic estimate of the advective scale of our study. Using the maximum tidal current velocities predicted during our study period (ebb and flood of 0.67 and 0.41 ms^{-1} , respectively, occurring on 8 August 2010, for a National Ocean Service tidal current station 4.2 km west of our study site), we estimate that our technique could integrate variation in water mass properties over a total distance of 11.0 km, i.e., up to 5.5 km on either side of the mooring location, along the primary east–west axis of tidal flow.

Correction for Air–Sea Gas Exchange

Because free water mass estimates of ecosystem metabolism are based on changes in concentration of a dissolved gas (i.e., O_2 or CO_2), the method also requires that one account for gain from or loss to the atmosphere across the air–water interface. We estimated this gain or loss in terms of an hourly flux, F , according to:

$$F = k_{\text{O}_2} \left[\frac{([O_2]_{\text{sat},t1} - [O_2]_{\text{obs},t1}) + ([O_2]_{\text{sat},t2} - [O_2]_{\text{obs},t2})}{2} \right] \quad (6)$$

where F is in units of grams of O_2 per square meter per hour and k_{O_2} is the gas transfer velocity in meters per hour. The bracketed term describes the average concentration gradient driving the flux over the course of each hour, where $[O_2]_{\text{sat},t1} - [O_2]_{\text{obs},t1}$ and $[O_2]_{\text{sat},t2} - [O_2]_{\text{obs},t2}$ are the differences between concentration at saturation and observed concentration (both in grams per cubic meter) at the beginning and end of each hour, respectively. We determined $[O_2]_{\text{sat}}$ according to Weiss (1970), based on our observations of salinity and temperature. A negative value of F in this case results when the water is supersaturated with respect to DO (i.e., $[O_2]_{\text{obs}} > [O_2]_{\text{sat}}$); the negative flux is net evasion, or diffusion of oxygen from the water to the atmosphere.

Estimation of Gas Transfer Velocity

The model used to calculate gas transfer velocity across the air–water interface (k_{O_2}) can significantly affect estimates of ecosystem metabolism in estuaries (see, e.g., sensitivity analyses in Caffrey 2004; Howarth et al. 1992). One must therefore carefully select an appropriate boundary-layer model and choose an appropriate method for estimating the velocity (Raymond and Cole 2001). Because our site draws aspects of its physical and biogeochemical character from both the coastal ocean and the shallower, more traditional estuary to its west, we estimated k_{O_2} as a function of wind velocity using three different parameterizations. The metabolic rates we report below are the mean values of the three independent estimates we obtained using the different models.

We first estimated k_{O_2} according to the cubic relationship of Wanninkhof and McGillis (1999)

$$k_{660} = 0.0283 \times U_{10}^3 \quad (7)$$

where U_{10} is the wind velocity normalized to a height of 10 m above the sea surface and k_{660} is the transfer velocity for carbon dioxide in seawater at 20 °C, which corresponds to a Schmidt number (Sc) of 660. We estimated U_{10} from our observations of wind speed at 3.5 m according to Panofsky and Dutton (1984). The parameterization in Eq. 7 is based on carbon dioxide covariance flux measurements in the open ocean.

We converted the velocity at $\text{Sc}=660$ to k_{O_2} at the Schmidt number for oxygen gas at the observed temperature and salinity, Sc_{O_2} , according to:

$$\text{Sc}_{\text{O}_2} = \frac{\eta}{\rho_{\text{SW}} D_{\text{O}_2}} \quad (8)$$

and

$$k_{\text{O}_2} = k_{660} \left(\frac{\text{Sc}_{\text{O}_2}}{\text{Sc}_{660}} \right)^n \quad (9)$$

where η is the dynamic viscosity in kilograms per meter per second (Sharqawy et al. 2010), ρ_{SW} is the density of seawater at the observed salinity, and temperature in kilograms per cubic meter, D_{O_2} is the mass diffusivity of oxygen gas in water in square meters per second according to Wanninkhof (1992) using the association factor of Hayduk and Laudie (1974), and n is the Schmidt number exponent. We applied an exponent of $-2/3$ for $U_{10} \leq 4.2 \text{ ms}^{-1}$ and $-1/2$ for $U_{10} > 4.2 \text{ ms}^{-1}$.

We also computed the gas transfer velocity according to the best-fit model of Raymond and Cole (2001)

$$k_{600} = 1.91 e^{0.35(U_{10})} \quad (10)$$

and the floating dome model of Marino and Howarth (1993) for oxygen gas in fresh water at 20 °C:

$$k_{530} = 1.09 + 0.249 \times U_{10} \quad (11)$$

Using the form of Eq. 9 with the appropriate Schmidt numbers, we converted the velocities obtained from these two models, $k_{\text{CO}_2,600}$ and $k_{\text{O}_2,530}$, respectively, to our desired k_{O_2} for measured salinity and water temperature.

Results

Nitrate

From our in situ spectrophotometric data (Fig. 2b), we obtained for the study period a mean nitrate concentration of 1.7 μmolL^{-1} and daytime mean concentration of

$1.4 \mu\text{molL}^{-1}$. These observations were consistent with the low concentrations we measured in our discrete samples, with annual data for central Long Island Sound dating back to 1992 (CTDEEP unpublished data; Fig. 4), and with previous observations of summer nutrient concentrations in the central Sound (Anderson and Taylor 2001; Bowman 1977; Chen et al. 1988; Riley and Conover 1956). Nitrate in the central Sound did not exceed a concentration of $3.9 \mu\text{molL}^{-1}$ at any time during the study period.

The nitrate results give us confidence that the SUNA is accurate to within $\pm 0.5 \mu\text{molL}^{-1}$ in coastal/estuarine waters characterized by minimal turbidity (calibration data not shown; discrete samples are plotted in Fig. 2b as open red circles). The SUNA proved capable of detecting relative changes on the order of $0.1 \mu\text{molL}^{-1}$ on scales > 12 h. While higher turbidity can decrease the accuracy of in situ optical nitrate measurements by up to $1.5 \mu\text{molL}^{-1}$ (e.g., Zielinski et al. 2011), our results are consistent with findings from other studies that have employed similar instruments in relatively clear waters (Christensen and Melling 2009; Johnson 2010; Johnson et al. 2006; Pidcock et al. 2010). Time-series analysis allowed us to isolate and quantify clear diel fluctuations in nitrate and DO (e.g., Fig. 3c), which were often partly obscured in the raw data by other dynamics that act on longer time scales, such as seasonal variation and mixing of multiple water masses (Fig. 2a, b).

Nitrogen Speciation

Nitrate comprised, on average, between 10 and 15 % of TDN within the water column at the site. This value, calculated from SUNA-derived nitrate concentrations and TDN measured in discrete samples at 11 dates over the course of the study period, was consistent with trends in speciation observed over the previous two decades (Fig. 4). By

contrast, only a very low fraction of water-column TDN (< 5 % on average) was present as total ammonia ($\text{NH}_3 + \text{NH}_4^+$). We did not consider any potential ammonia fluxes from underlying sediments at the site.

Because each species of algae is necessarily adapted to exploit different proportions of the various forms of nitrogen, the nature and severity of eutrophication often hinges not merely on the total quantity of anthropogenic nitrogen export but on the form in which it is delivered to a particular ecosystem (Paerl and Piehler 2007). The low abundance of both dissolved inorganic species relative to TDN suggests that in central Long Island Sound, as elsewhere, most dissolved nitrogen was present as dissolved organic nitrogen (DON). While certain species of cyanobacteria, diatoms, and heterotrophic dinoflagellates can in some instances assimilate DON directly during cell growth (Antia et al. 1991), most DON present in the oceans is in complex macromolecules not readily accessible to phytoplankton engaged in the fixation of organic matter (McCarthy et al. 1997). In considering here the potential enrichment of phytoplankton populations, we thus focus our attention on the dissolved inorganic forms, with particular emphasis on partitioning between the two species.

The inorganic nitrogen speciation we observed at the study site is consistent with the general profile of anthropogenic nitrogen input to Long Island Sound, which is comprised predominately of discharges from wastewater treatment facilities. Various estimates put the relative magnitude of these WWTP inputs at between 40.1 % (NYSDEC and CTDEP 2000) and 56.7 % (Castro et al. 2003) of the total Long Island Sound nitrogen load. Generally, in urbanized watersheds such as those responsible for much of the drainage to the Sound, nitrate often comprises a higher percentage of the total nitrogen load relative to ammonia. Nitrate predominates in the non-point sources (e.g., impervious surface runoff) and

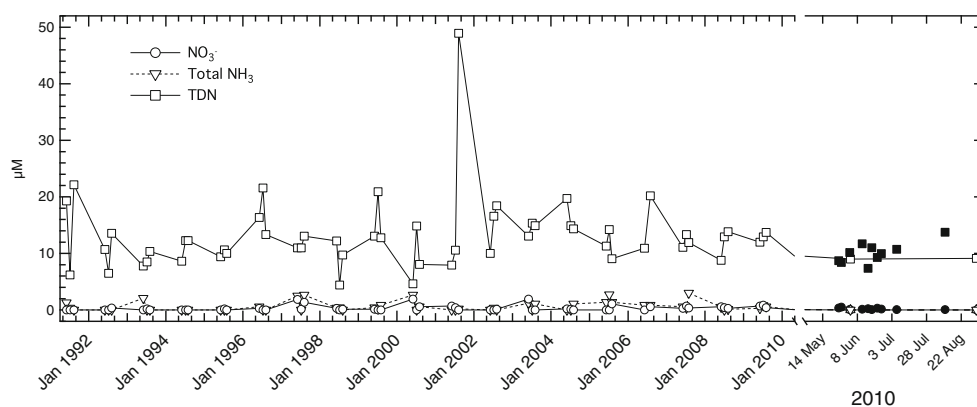


Fig. 4 Interannual trends in the concentrations of bioavailable nitrogen species as a fraction of total dissolved nitrogen (TDN) at the study site in central Long Island Sound from 1992 to 2010, as measured in discrete samples. *Open markers* are from the CTDEEP (formerly

CTDEP) monthly sampling program at station I2 (Matthew Lyman, unpublished data). The *closed markers* in the rightmost section of the plot are results from this study; note the expanded *x-axis*. All samples were taken during daylight hours

wastewater treatment discharges that are the primary inputs to these systems. Conversely, in watersheds dominated by intensive livestock agriculture, a greater proportion of the total nitrogen load often comes in reduced forms such as ammonium and organic nitrogen (Paerl and Piehler 2007). Notably, only 15.4 % of the total Long Island Sound nitrogen load originates in agriculture; by comparison, agricultural activities in the Chesapeake Bay watershed, including intensive poultry feeding operations, are responsible for more than 53 % of the total nitrogen load (Castro et al. 2003).

The observed speciation is also supported by direct evidence and $\delta^{15}\text{N}$ – $\delta^{18}\text{O}$ isotopic analysis from examination of several Long Island Sound wastewater treatment discharges to the Naugatuck and Quinnipiac rivers (Anisfeld et al. 2007). The vast majority of plants that discharge to the Sound are secondary treatment facilities that accomplish only nitrification, the conversion of ammonia, which is generally toxic, to nitrate. A very limited number of facilities that discharge to the Sound are equipped to accomplish any significant denitrification, a microbially catalyzed tertiary treatment process that converts nitrate to nonreactive dinitrogen gas (N_2); only this process reduces the total amount of nitrogen that ends up in receiving waters. This distribution of treatment capacity produces an aggregate end-member nitrogen discharge stream composed overwhelmingly (i.e., >80 % of TDN) of nitrate (Anisfeld et al. 2007).

Production and Respiration

Net Community Productivity

Daily rates of all five measures of ecosystem metabolism ranged considerably, often changing from one day to the next by an order of magnitude (Table 1; Figs. 5 a and 6a). Daily, depth-integrated rates of daytime net community production ranged from $-2,880$ to $4,460 \text{ mgCm}^{-2}\text{day}^{-1}$; the mean rate of NCP_d (± 95 % CI) during the study period was $1,100 \pm 208 \text{ mgCm}^{-2}\text{day}^{-1}$ (Table 2). That the two daily rate extremes occurred on adjacent dates (10 and 9 June, respectively) suggests that large metabolic variation can occur over very short time scales. The 9 June NCP_d maximum coincides with a maximum in observed chlorophyll fluorescence corresponding to a peak chlorophyll *a* concentration of $6.8 \mu\text{gL}^{-1}$ (Fig. 5c). Day-to-day variations of similar magnitude have been observed in daytime ecosystem production rates in Long Island Sound (Anderson and Taylor 2001), in other temperate estuaries (D'Avanzo et al. 1996), and in offshore ecosystems (DeGrandpre et al. 1997).

The rate of community productivity increased steadily over the course of the spring and summer study period from a mean of $672 \pm 531 \text{ mgCm}^{-2}\text{day}^{-1}$ in May to a mean of $1,650 \pm 478 \text{ mgCm}^{-2}\text{day}^{-1}$ in August (the average rates ± 95 % CI for June and July were $1,200 \pm 444$ and $1,010 \pm 214 \text{ mgCm}^{-2}$

day^{-1} , respectively). The difference between the May and August monthly mean values was significant ($p < 0.05$; paired *t* test). The average hourly net community production rate was weakly correlated with average temperature, suggesting at least some of the increase in NCP_d was driven by the steady rise in sea surface temperature (Fig. 2e) typical of Long Island Sound and other temperate estuaries in summertime ($R^2 = 0.12$; $p = 0.002$).

Community Respiration

Rates of community respiration, R_c , also varied widely over daily timescales (Fig. 6a). A maximum, depth-integrated daily respiration rate of $6,240 \text{ mgCm}^{-2}\text{day}^{-1}$ was observed during the final weeks of the study period on 6 August, when surface temperatures were the highest. The mean community respiration rate for the study period was $1,660 \pm 431 \text{ mgCm}^{-2}\text{day}^{-1}$. As in the case of net community production, the respiration rate increased over the course the study period from a monthly mean of $257 \pm 1,630 \text{ mgCm}^{-2}\text{day}^{-1}$ in May to a mean of $2,650 \pm 1,340 \text{ mgCm}^{-2}\text{day}^{-1}$ in August. Much of this increase appeared to be driven by seasonal warming (Fig. 2e); the average hourly respiration rate was weakly correlated with sea surface temperature ($R^2 = 0.13$; $p < 0.001$).

The respiration rates we present fall well within the range of previous measurements of ecosystem metabolism in Long Island Sound (Anderson and Taylor 2001; Goebel et al. 2006) and in other temperate estuaries (Caffrey 2004; Kemp et al. 1997); our findings agree generally with these previous measurements despite significant differences in the methods used (Table 3). As in the case of daytime net production, estuaries exhibit significant day-to-day variation in rates of community respiration. This is particularly true at elevated summertime temperatures of systems that experience large anthropogenic inputs of nutrients and organic matter (Caffrey 2003; D'Avanzo et al. 1996; Zhang et al. 2010). Goebel and Kremer (2007) ascribed variation in respiration rates in Long Island Sound to factors such as light availability (particularly in late summer) and standing chlorophyll concentration.

Gross Primary Productivity

Rates of gross primary productivity ranged from near zero at the outset of the study period (2 days in May) to a maximum of $6,390 \text{ mgCm}^{-2}\text{day}^{-1}$ on 22 July. The mean rate of GPP (± 95 % CI) for the study period was $2,080 \pm 419 \text{ mgCm}^{-2}\text{day}^{-1}$. These rates agree with previous summertime and annual estimates of GPP in Long Island Sound and in other temperate estuaries of similar size (Table 3). Monthly mean rates for May, June, July, and August were, respectively, $563 \pm 1,450$, $2,160 \pm 718$, $2,210 \pm 494$, and $3,150 \pm 1,140 \text{ mg}$

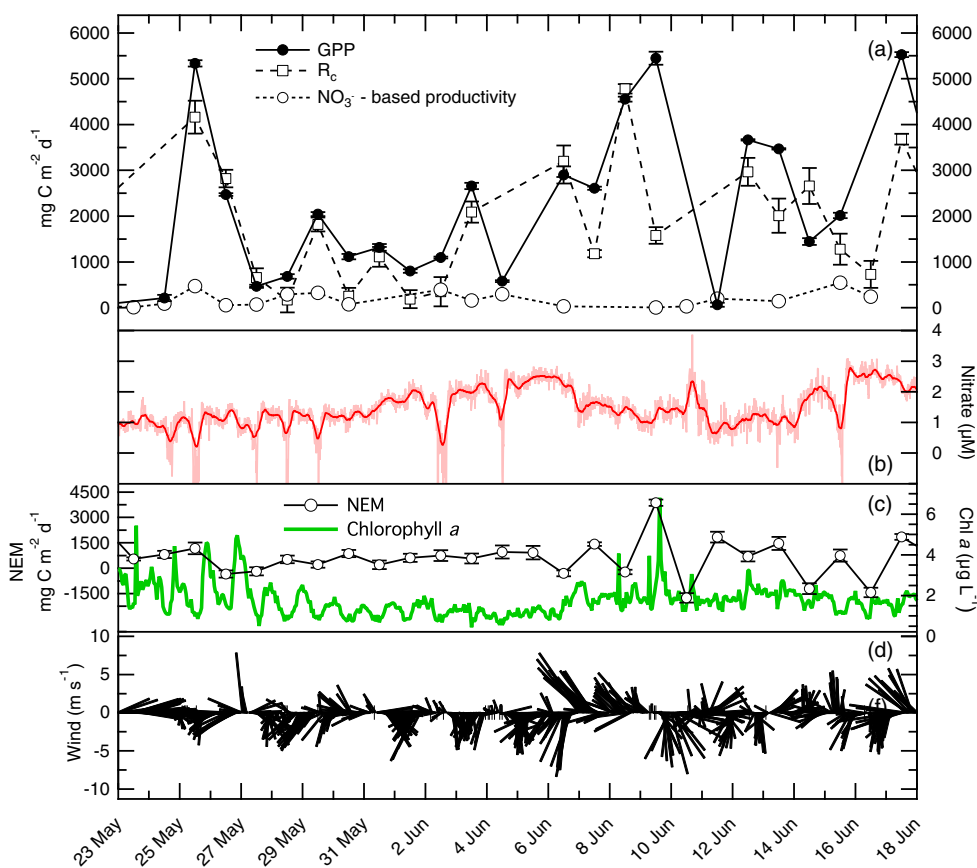
Table 1 Representative daily variation in primary study parameters over two periods in central Long Island Sound

Date (2010)	Productivity ($\text{mgCm}^{-2}\text{day}^{-1}$)		R_c ($\text{mgCm}^{-2}\text{day}^{-1} \pm 95\text{ CI}$)	NEM ($\text{mgCm}^{-2}\text{day}^{-1} \pm 95\text{ CI}$)	Average surface wind speed ($\text{ms}^{-1} \pm \text{SD}$)	Total F ($\text{mgCm}^{-2}\text{day}^{-1}$; $F < 0$ indicates water is supersaturated and flux is thus from sea to air)		f ratio (NO_3^- based new production/ NCP_d)		
	GPP ($\pm 95\text{ CI}$)	NO_3^- based new production ^a				Wamminkhof and McGillis (1999)	Raymond and Cole (2001)		Marino and Howarth (1993)	Mean of three models ($\pm 95\text{ CI}$)
24 May	210±69	87.3	-600±143	810±212	3.6±1.3	-100	-370	-340	-271±167	0.15
25 May	5,330±67	471.1	4,160±356	1,170±344	2.2±1.2	-110	-570	-600	-425±312	0.17
26 May	2,470±29	57.0	2,820±190	-350±206	4.5±1.0	-490	-1,290	-1,080	-952±474	0.08
27 May	470±32	-	660±204	-190±235	3.6±1.6	-240	-710	-610	-519±284	-
28 May	680±48	289.7	170±270	520±233	3.0±1.8	-230	-730	-660	-541±311	0.50
29 May	2,040±43	325.3	1,820±152	220±191	3.9±2.0	-350	-900	-730	-659±323	0.36
30 May	1,120±59	74.6	250±182	870±215	3.3±1.0	-130	-490	-470	-362±230	0.08
31 May	1,320±76	-	1,110±216	210±255	3.9±1.7	-350	-950	-800	-702±357	-
1 Jun	800±39	-	190±198	620±235	3.6±1.9	-390	-1,060	-860	-772±389	-
2 Jun	1,090±20	395.6	350±321	750±324	2.5±1.4	-160	-650	-640	-485±314	0.45
3 Jun	2,660±67	159.8	2,090±233	570±292	3.5±1.4	-310	-990	-900	-734±419	0.12
4 Jun	580±17	293.3	-370±379	950±387	2.7±1.8	-290	-960	-890	-715±416	0.36
6 Jul	850±36	-	440±113	650±125	2.4±0.5	-40	-280	-290	-203±161	-
7 Jul	2,970±46	-	1,240±137	2,770±155	2.5±1.1	-90	-400	-400	-293±204	-
8 Jul	1,470±28	-	1,280±171	300±312	4.0±0.9	-250	-750	-660	-554±301	-
9 Jul	2,440±26	-	900±145	2,460±269	3.6±0.8	-250	-860	-790	-636±378	-
10 Jul	2,350±5	-	1,260±172	1,740±271	2.6±1.1	-100	-520	-530	-384±278	-
11 Jul	1,210±16	-	1,020±185	300±290	4.0±1.1	-340	-1,010	-880	-746±401	-
12 Jul	810±92	-	270±195	860±294	3.8±1.3	-350	-1,040	-900	-764±413	-
13 Jul	1,920±28	-	1,460±127	750±160	4.3±1.7	-490	-1,280	-950	-907±452	-
14 Jul	2,160±62	-	870±71	2,090±209	3.3±1.9	-290	-810	-680	-595±306	-
15 Jul	730±45	-	580±116	240±168	3.2±1.7	-80	-300	-280	-221±139	-

Presented are rates of gross primary production (GPP), NO_3^- based new production, daytime net community production (NCP_d), community respiration (R_c), net ecosystem metabolism (NEM), average surface wind speed, and the total daily air–sea gas flux (F) calculated using each of the three gas exchange models. Differences between the three air–sea gas exchange models were used to generate confidence intervals for the ecosystem metabolism figures. The f ratio is calculated for the May and June dates. Parameters were calculated as described in Tables 1 and 2. All values are reported as depth-integrated values of milligrams of C or milligrams of O₂ per square meter per day for entire water column. Where necessary, to convert O₂-based measurements to units of C, we assumed a photosynthetic quotient of 1.2 (1.2 mol O₂:1 mol CO₂). To convert parameters based on ΔNO_3^- , we assumed Redfield stoichiometry (6.6 mol C/mol N)

^a NO_3^- based production could not be calculated for days on which the diel NO_3^- flux was decoupled from the daily production cycle, i.e., the pairing between PAR and dissolved oxygen production; see text for explanation. On these days, we hypothesize that some other variable, e.g., tidal currents or wind forcing, caused perturbations in NO_3^- concentration that masked the underlying diel signal, making it impossible to accurately determine rates of new production

Fig. 5 Daily rates of **a** community respiration, R_c , and new production based on nitrate, as a fraction of gross primary productivity over a 3-week segment of the study period in 2010. Variations in these three parameters reflect daily and longer-term changes in **b** nitrate concentration, **c** chlorophyll *a* (a proxy for the standing crop of biomass), and **d** wind speed and direction. Error bars in *a* and *c* represent 95 % confidence intervals



$\text{Cm}^{-2}\text{day}^{-1}$. In spite of these general trends, rates of GPP, like rates of NCP_d and R_c , varied considerably from day to day (Fig. 6a).

Net Ecosystem Metabolism

Large day-to-day variations in the rate of ecosystem metabolism, a fundamental measure of the balance between respiration and photosynthesis, reflected the significant

variations evident in rates of R_c , NCP_d , and GPP (Fig. 6b). Rates of NEM ranged from $-2,940 \text{ mgCm}^{-2}\text{day}^{-1}$ on 21 May to a maximum of $3,870 \text{ mgCm}^{-2}\text{day}^{-1}$. While the mean rate for the study period ($426 \pm 203 \text{ mgCm}^{-2}\text{day}^{-1}$) indicated the system remained weakly autotrophic at seasonal timescales, the mean rate for July ($292 \pm 235 \text{ mgCm}^{-2}\text{day}^{-1}$) was effectively zero, suggesting conditions at the site trended toward near trophic balance or heterotrophy as the summer progressed.

Fig. 6 Significant variation in daily rates of **a** gross primary productivity and community respiration and **b** net ecosystem metabolism in central Long Island Sound during the summer and spring 2010. NEM is the balance between the two other variables. A *negative value* reflects net heterotrophy, i.e., the respiration of more organic matter than is being produced by autochthonous sources. A *positive value* indicates the system is net autotrophic

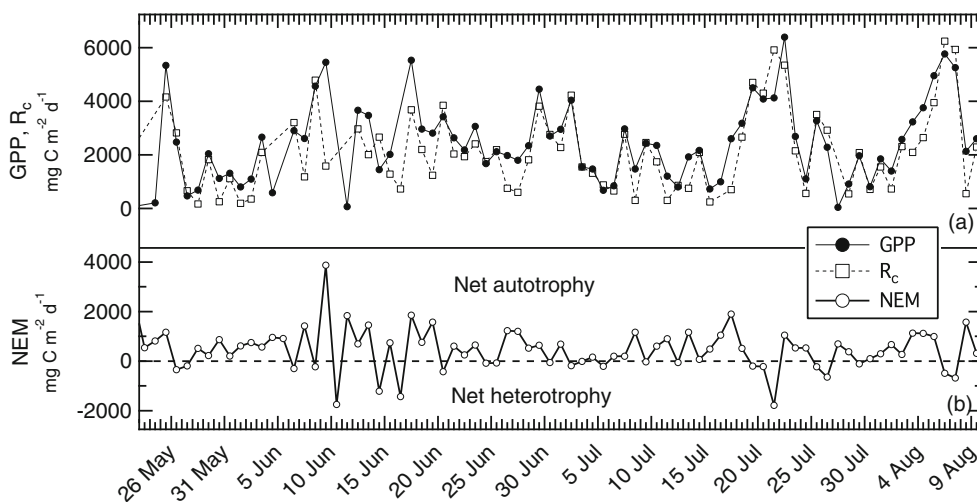


Table 2 Mean depth-integrated values of community metabolic parameters at central Long Island Sound, May–August 2010

Parameter (U)	Mean value ($\pm 95\%$ CI)	Basis
Hourly respiration, R_h ($\text{mgCm}^{-2}\text{h}^{-1}$)	69.1 ± 17.9^a	High-frequency overnight measurements of ΔO_2 , corrected for air–sea exchange
Gross community respiration, R_c ($\text{mgCm}^{-2}\text{day}^{-1}$)	1660 ± 431^a	$R_h \times 24$ (rate assumed to be constant over 24-h period)
Daytime net community production, NCP_d ($\text{mgCm}^{-2}\text{day}^{-1}$)	1100 ± 208^a	High-frequency daytime measurements of ΔO_2 , corrected for air–sea exchange
Gross primary production, GPP ($\text{mgCm}^{-2}\text{day}^{-1}$)	2080 ± 419^a	$\text{GPP} = \text{NCP}_d + R_h \times \text{hours of daylight}$
Net ecosystem metabolism, NEM ($\text{mgCm}^{-2}\text{day}^{-1}$)	426 ± 203^a	$\text{NEM} = \text{GPP} - R_c$; a positive value is net autotrophy
New production, i.e., phytoplankton growth based on NO_3^- uptake, P_{NO_3} ($\text{mgCm}^{-2}\text{day}^{-1}$)	182 ± 37^b	Hourly fluxes from high-pass filtered $[\text{NO}_3^-]$
f ratio, i.e., ratio of NO_3^- based production to production based on all forms of fixed N (Eppley and Peterson 1979)	0.25^b	$\text{P}_{\text{NO}_3} / \text{NCP}_d$

For ease of comparison, all values are reported in units of milligrams of C. To convert O_2 -based measurements to units of C, we assumed a photosynthetic quotient of 1.2 (1.2 mol O_2 :1 mol CO_2). To convert parameters based on ΔNO_3^- , we assumed Redfield stoichiometry (6.6 mol C/mol N).

^a Mean for May–August

^b Mean for May–June

Discussion

Controls on Nitrate Concentration and Uptake

Timescales of Hours to Days: Cyclical and Recurring Controls

As is true in most natural systems, nitrate concentrations in central Long Island Sound were correlated to a variety of physical and biological forces that acted over different timescales. On timescales of hours to days, variation in surface-layer nitrate concentrations was dominated by the central biological processes of photosynthesis and respiration. The high-frequency data show a daily, cyclical rise and fall that is strongly coupled to the diel photosynthetic cycle (Fig. 3); the cyclical trend in the nitrate signal is enhanced by applying a high-pass filter to the data (Fig. 3c). Quantitatively, the daily average dissolved oxygen concentration, a proxy for the relative balance on any given day between photosynthesis and respiration, was the single most significant predictor of nitrate over the course of the study period, explaining 59 % of the variation in observed concentrations of the nutrient (Fig. 7a; $p < 0.001$).

The lowest nitrate concentrations, often reaching levels below the detection limit of the SUNA, were typically observed in midafternoon, coinciding with daily peaks in irradiance and dissolved oxygen production, indicators of maximum photosynthetic activity. The highest concentrations were typically observed in the very early morning hours after the surface-layer nitrate inventory was replenished overnight from a nitrate reservoir of slightly higher concentration

below the mixed layer. This pattern, in which daytime photosynthetic assimilation of nitrate by phytoplankton results in a sharp drawdown in concentration that is counterbalanced by nighttime recharge through tidal advection and diffusion, has been observed in previous time-series studies using similar instruments in waters with higher absolute nitrate concentrations (Johnson 2010; Johnson et al. 2006; Zielinski et al. 2011).

The data presented here suggest nitrate concentrations at the site often averaged between 1 and 2 μmolL^{-1} over the course of a 24-h day. We do not believe these observations are necessarily incompatible with the zero or near-zero summer nitrate concentrations recorded for the central Sound in previous studies (Bowman 1977; Riley and Conover 1956) and by the CTDEEP monthly sampling program (CTDEEP unpublished data), which have analyzed discrete samples using traditional colorimetric methods. Sample collection in these previous studies has traditionally been performed during daylight hours when nitrate concentrations are lowest; few samples have been collected during the early morning, when concentrations appeared to hit their maximum on many days during this study. We suggest that these previous studies may have underestimated daily average nitrate concentrations in the central Sound by 1 or 2 μmolL^{-1} .

The horizontal advection of water masses due to tidal transport also appeared to produce some variation in nitrate over daily and hourly timescales. Decoupling of the nitrate signal from the photosynthetic cycle (i.e., distortion of the signal so that the diurnal pattern of photosynthesis is not evident) often coincided with stronger than average tidal currents during spring tides at Sachem Head, the nearest station for which

Table 3 Estimates of community metabolic rates at selected locations in Long Island Sound and in two other estuaries

Study location	Productivity (mgCm ⁻² day ⁻¹ ±95 % CI)		Community respiration (mgCm ⁻² day ⁻¹ ±95 % CI)	Method	Reference
	Gross	Net community or net primary metabolism ^a			
Central Long Island Sound, spring–summer 2010	2,080±419	1,100±208 ^e	1,660±431	High-frequency ΔO ₂ in free water mass, corrected for air–sea gas exchange	This study
Central-west Long Island Sound at station H4, approximately 14 km south of New Haven, spring–summer, 2002–2003	2,620±900	–	–	O ₂ -based light/dark bottle incubations, depth integration using photosynthesis-irradiance curves	Goebel et al. 2006
Central-west Long Island Sound, ranges of monthly averages at 8 stations to west of longitude 72°40'W, 2002–2003	40 (±110) to 17,300 (±6,100) ^b	–12,500 (±2,700) to 11,600 (±11,000) ^{b,c}	–500 (±300) to 16,600 (±2,700) ^b	O ₂ -based light/dark bottle incubations, depth integration using photosynthesis-irradiance curves	Goebel et al. 2006
Western Long Island Sound near mouth of East River at Throgs Neck, summer, 1992–1993	–	0 to 37,000 molCm ⁻² day ⁻¹ ^d	–	Dilution-culture incubations; rates extrapolated from change in chl <i>a</i> concentration	Anderson and Taylor 2001
Narragansett Bay, RI, at T-Wharf, S end Prudence Island, annual average, 1995–2000	2,500±310 ^e	–	2,900±380 ^e	High-frequency ΔO ₂ in free water mass, corrected for air–sea gas exchange	Caffrey 2004
Waquoit Bay, MA, at Central Basin, annual average, 1995–2000	2,100±94 ^e	–	2,800±130 ^e	High-frequency ΔO ₂ in free water mass, corrected for air–sea gas exchange	Caffrey 2004
Chesapeake Bay, lower section (polyhaline; to south of latitude 38°N), annual average, 1990–1992	1,670 ^f	–	1,460 ^f	O ₂ -based light/dark bottle incubations, depth integration using photosynthesis-irradiance curves	Kemp et al. 1997

All estimates except those presented in the current study are reported as depth-integrated values of C per square meter per day for the water column; our estimates are integrated measurements for the euphotic zone. Where necessary, to convert O₂-based measurements to units of C, we assumed a photosynthetic quotient of 1.2 (1.2 mol O₂:1 mol C)

^a Defined as the balance between gross primary (autotrophic) production and community respiration, i.e., GPP–R_c; a value <0 indicates net heterotrophy while a positive value indicates net autotrophy

^b Peak rates of GPP and NCP were observed in summer at the extreme western end of LIS; peak rate of R_c was observed in summer at station E1

^c Reported as net community productivity (NCP)

^d Reported as net primary productivity (NPP)

^e Values reported as ±SE

^f Estimates of annual rates (square meters per year) were converted to daily rate estimates by dividing by 365; peak values of GPP (~5,000 mgCm⁻² day⁻¹) were observed in the Lower Bay in July

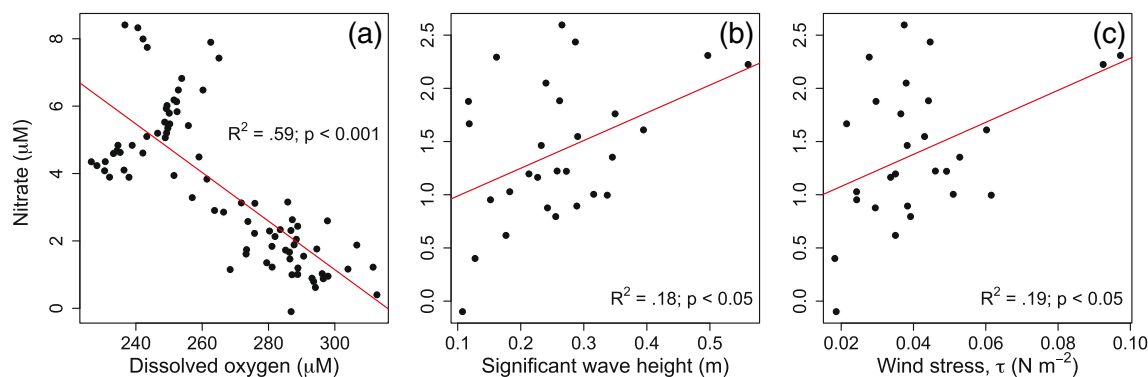


Fig. 7 Relative contributions of three parameters to overall variation in the nitrate signal during a segment of the study period from 23 May to 30 June 2010. In **a** nitrate concentrations averaged over each 12-h period are plotted versus average dissolved oxygen concentrations. In

b and **c**, nitrate is plotted versus significant wave height and wind stress. *Red lines* were fitted by linear least-squares regression. The relationship in each pairing was significant ($p < 0.05$)

predictions are made (data not shown). Elsewhere in Long Island Sound, tidal advection promotes the horizontal movement of water masses with significantly different chemical properties (O'Donnell et al. 2008).

Seasonal-Scale Controls

On monthly to seasonal timescales, nitrate concentrations were controlled by changes in the structure and physical properties of the estuarine water column. A typical water-column stratification regime developed in the central Sound over the course of the study period (data not shown), though storm events frequently served to temporarily weaken the stratification regime and permit mixing across the thermocline. Conservative profiles of both temperature and salinity on 27 May suggest that stratification did not begin to develop at the site until early June. A deepening of the thermocline in mid-June was followed by establishment of a deep, well-formed thermocline by early July. The mean summertime nitrate concentrations of less than $2 \mu\text{molL}^{-1}$ during this period are typical of surface waters throughout much of Long Island Sound following the stratification onset and intensification that occurs in the late spring (Anderson and Taylor 2001; Bowman 1977). Only at stations in the extreme western reaches of the Sound (i.e., approaching New York City and its immediate environs) are surface concentrations in excess of $5 \mu\text{molL}^{-1}$ routinely observed in summertime (Bowman 1977).

Intermittent Control by Wind Forcing

While the photosynthetic cycle and other recurring controls appeared to explain the majority of variation in nitrate concentration, wind stress was also a powerful intermittent physical forcing that acted to modify the principal nitrate trend component significantly and often unpredictably. In

the absence of significant storm activity or changes in prevailing weather, winds were generally weakest in early morning and strongest and most variable in the late afternoon, when a sea-breeze predominated. Winds varied in direction, with minor storm events occurring on 7, 10, and 17 June (Fig. 5), on 14–15 and 22 July, and on 4–5 August. These storms were accompanied by moderate rainfall (Fig. 2). Although no large storms occurred during the study period, wind forcing had a significant effect on surface-layer nitrate concentrations through both its variable daily behavior and during more pronounced intermittent storm events.

The large dataset we acquired through sustained, high-frequency sampling allowed us to quantitatively assess the effect of wind stress on nitrate uptake at the site over an extended period. As expected, on a daily basis, more pronounced wind stress generally increased surface layer nitrate stocks through vertical mixing. Wind stress explained a significant ($p < 0.05$) albeit modest proportion of the overall variation in nitrate concentration. Wind alone explained 19 % of the overall variation, while significant wave height, measured independently though largely a function of surface wind speeds, explained 18 % of the variation (Fig. 7b, c). On days with higher winds, more nitrate was presumably entrained from below the mixed layer, consistent with the classical conception of wind-driven nutrient entrainment (see, e.g., Klein and Coste 1984). The rapid response of surface-layer nitrate concentrations to wind forcing has been previously observed in oligotrophic zones of the open ocean: In several observational studies, sustained winds entrained nitrate and other nutrients from below a heavily depleted mixed layer, causing measureable increases in nutrient concentrations followed by drawdown as the nutrients were assimilated by phytoplankton (Eppley and Renger 1988; Klein and Coste 1984; Marra et al. 1990). In LIS, wind-induced vertical mixing is the primary mechanism by which dissolved oxygen is exchanged in summer between surface and subpycnocline waters

(O'Donnell et al. 2008). This same vertical mixing explains the exchange of nitrate and other species across the pycnocline.

While wind stress generally had an effect consistent with that observed in the open ocean, we observed during a nighttime storm event on 7 June an intriguing ecosystem response inconsistent with the general model (Fig. 8). During the event, wind-induced deepening of the mixed layer resulted in rapid loss of surface-layer nitrate stocks that had accumulated during a period of relatively calm winds over the previous week. On the days leading up to the storm event, we observed the characteristic, photosynthetically driven daily oscillations in both nitrate and dissolved oxygen concentration that were evident throughout the study period. This pattern of diel rise and fall (solid red trace in Fig. 8) was accompanied by a gradual accumulation of both dissolved oxygen and nitrate that extended over a time period of several days (broken red trace). Following the rapid decrease in surface-layer concentration caused by the event, continued wind forcing appeared to perturb or mask the regular photosynthetic cycles in both species for several days.

In reconciling this event with our statistical analysis, we note that the classic wind stress-entrainment response model is not universally applicable. Nutrient entrainment through surface wind forcing occurs only if winds are sufficiently strong and long in duration and only if the water column is not so strongly stratified that it resists mixing (Bigg et al. 1989). Additionally, because bottom-layer nitrate concentrations in the central Sound are not generally any appreciably higher than concentrations at the surface during summer months (Matthew Lyman, CTDEEP, unpublished data), nitrate is not necessarily entrained into the mixed layer even when stratification is weakened by wind stress.

No Correlation with Rainfall

Unexpectedly, we did not find any significant statistical relationship between surface-layer nitrate concentrations and rainfall. Evidence suggests that atmospheric deposition can be significant source of anthropogenic ammonium and nitrate species ($\text{NO}_3^- + \text{HNO}_3$) to the overall LIS DIN pool (Hu et al. 1998; Luo et al. 2002). Deposition has been previously linked to surface-layer nutrient increases over short time scales in western Long Island Sound (Anderson and Taylor 2001). Relative to other inputs, however, the atmospheric input of all forms of nitrogen to Long Island Sound is estimated to be small (<13 % of the total load; NYSDEC and CTDEP 2000). Furthermore, many of the observed increases in ambient nitrate concentrations associated with rainfall in these previous studies were attributed not to direct wet deposition, but largely to the ensuing pulse in stormwater runoff and (untreated) sewage discharge that usually accompany large storm events in urbanized areas (Anderson and Taylor 2001). Because of our study site's relative distance from land, we hypothesize that, at least over short time scales, it should be somewhat more buffered with respect to these discharges than is the western Sound.

Estimates of New Production and the f Ratio

Given the apparent nitrogen speciation at our site, the relatively small magnitude of the atmospheric nitrogen input, and evidence that very little of the primary anthropogenic input to Long Island Sound (i.e., wastewater) was as ammonium, we approximate total new production here as the rate of fixation of new biomass based on allochthonous

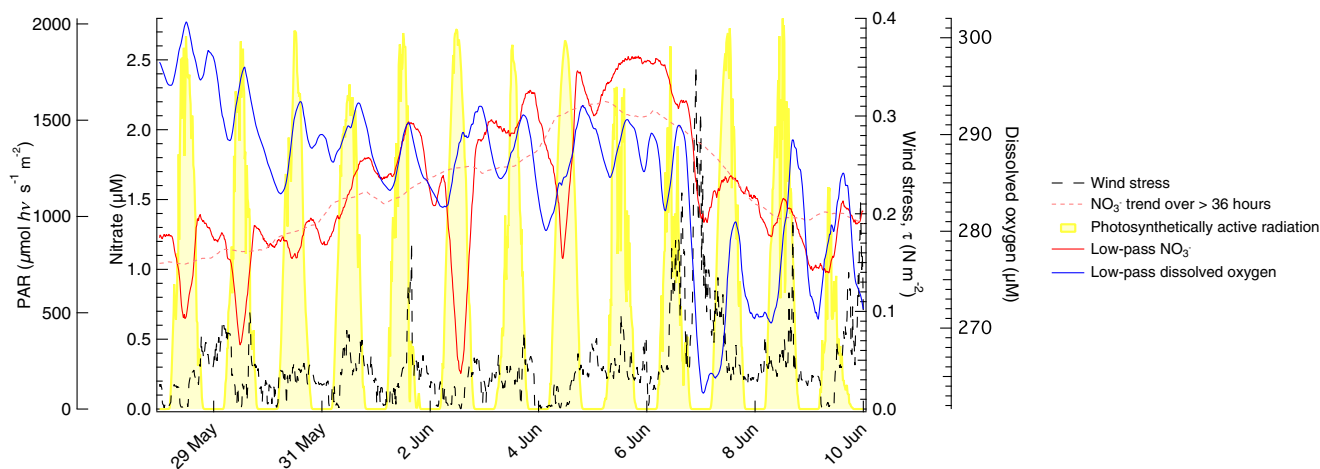


Fig. 8 Dissipation of accumulated nitrate stock through deepening of mixed layer, immediately following the onset of a wind event during the night of 8 June 2010. A similar drop in surface DO concentration is also evident during the event, as oxygen in the well-ventilated surface water is exchanged with the oxygen-depleted bottom layer. Wind velocities observed during this storm event were the highest observed

during the study period. The *solid red line* includes only components of the nitrate signal with periods >2 and <25 h; very short-term variability and the longest period signals were eliminated from this spectral subset using a band-pass Fourier transform. The *broken red line* is the product of a low-pass filter; this subset includes only cycles with periods >25 h

nitrate. This is the simple, original definition of Dugdale (1967) as modified by Eppley and Peterson (1979). In the case of the mesotrophic and oligotrophic open-ocean systems in which the concept of new production was conceived, nitrate is assumed to be allochthonous because it is delivered to the surface layer from below the thermocline. In the case of estuaries such as Long Island Sound, a significant fraction of the allochthonous nitrate may also be delivered from lateral terrestrial inputs that are either natural or anthropogenic.

For the subset of the study period for which we had reliable nitrate data, rates of new production in the central Sound ranged from near-zero ($\sim 10 \text{ mgCm}^{-2}\text{day}^{-1}$ on 23 May) to a maximum of $546 \text{ mgCm}^{-2}\text{day}^{-1}$ on 15 June. The mean new production rate was $182 \pm 37 \text{ mgCm}^{-2}\text{day}^{-1}$, well above the $102 \text{ mgCm}^{-2}\text{day}^{-1}$ estimated by Eppley and Peterson (1979) for the world's inshore waters but lower than their accompanying estimate for neritic waters of $460 \text{ mgCm}^{-2}\text{day}^{-1}$.

Statistically significant changes in amplitude of the nitrate signal were not always evident in the high-pass dataset. On approximately 18 % of days, nitrate appeared to be decoupled from the photosynthetic cycle and a distinct rise and fall could not be discerned; on these days, rates of nitrate-based production were not calculated. The degree of decoupling, i.e., the extent to which the nitrate signal diverged from the regular daily pattern, appeared to be a function of wind and tidal strength. Strong winds and stronger than usual tides seemed to promote divergence, while the nitrate signal was more evident on days when meteorological and physical forces were weak.

Daily values of the f ratio, i.e., the ratio of new production to production based on all forms of fixed nitrogen

$$f = \frac{P_{NO_3}}{NCP_d} \quad (12)$$

ranged from near zero on several dates to a maximum of 0.50 on 28 May. The study period average f ratio of 0.25 is of the same order as values obtained for other temperate estuaries and approximately equal to the Eppley and Peterson (1979) global estimate for inshore waters (Table 4). The only other published f ratio estimate using nitrate data from an in situ spectrophotometer (0.68 ± 0.12) is for a coastal ocean station 20 km west of Monterey Bay, California, which is not biogeochemically or physically similar to our study site (Johnson et al. 2006). f ratio values in the literature are traditionally defined as a fraction of ^{14}C primary productivity, as is the estimate we cite here for the station west of Monterey Bay. In recognition of the fact that rates obtained from the ^{14}C method are generally thought to represent something between net and gross primary production (Marra 2009), we defined our f ratio as a fraction of net community production (NCP_d) rather than GPP .

We note here that the classic definition of new production neglects the processes of nitrogen fixation (Paerl 1997),

direct uptake of DON (Bronk et al. 1994), and surface-layer nitrification (Yool et al. 2007). Depending on their magnitude and significance to the particular ecosystem, the failure to include these processes may result in over- or underestimation of the rate of new production and thus the f ratio. The definition we adopt also neglects the fact that in estuaries specifically, ammonium may come from both allochthonous and autochthonous sources, making it a possible additional basis for new production (Mortazavi et al. 2000a; Paerl 1997).

The apparent biogeochemistry at our study site and the general nature of nitrogen enrichment in Long Island Sound suggest that the Eppley and Peterson definition should provide an adequate approximation of the rate of new production in central Long Island Sound. In other estuaries for which estimates of new production have been made, such as Apalachicola Bay, a shallow estuary in Florida that receives more than 72 % of its nitrogen load from agricultural activities (Castro et al. 2003), an approximation neglecting the ammonia species would very likely underestimate the rate of new production. In Apalachicola Bay, average annual new production was estimated to be $143 \text{ mgCm}^{-2}\text{day}^{-1}$ using a mass-balance nutrient model and primary productivity estimates from ^{14}C incubations (Mortazavi et al. 2000a). The f ratio we present here of 0.25 suggests that even at low concentrations, nitrate drives a very significant fraction of total production in central Long Island Sound.

Effect of Wind Forcing on New Production and the f Ratio

Wind forcing had a significant effect on both the rate of new production ($R^2=0.49$; $p<0.005$) and on the f ratio ($R^2=0.30$; $p<0.05$). Even as higher wind velocities increased surface-layer nitrate stocks, the forcing appeared to drive down the rate of new production and the value of the f ratio (Fig. 9). These relationships suggest that the delivery of nitrate to the surface layer is not alone sufficient to support an increase in primary production: Winds must be of appropriate strength and duration for the particular stratification regime and in an open ocean setting, also be accompanied by sufficient Ekman pumping. In two instances, a measureable bloom in primary production was observed only after a succession of separate wind events occurred over span of multiple days (Andersen and Prieur 2000; Wu et al. 2008). In Long Island Sound specifically, Chen et al. (1988) have suggested that nutrient entrainment and any resultant increase in primary production may result only from a combination of surface wind stress and tidal advection.

The fact that different physical mechanisms govern nutrient delivery to the mixed layer in the open ocean and in coastal environments and estuaries (Klein and Coste 1984)

Table 4 Estimates of the *f* ratio and gross versus new productivity for selected ecosystems and marine ecosystem types

Water body	Productivity ^a (mgCm ⁻² day ⁻¹ , unless noted, ±95 % CI)		<i>f</i> ratio	Method		Reference
	Total	New		Total production	New production	
Atlantic Ocean, modeled annual average ^b	286	71	0.26	¹⁴ C uptake method	¹⁵ N-labeled NO ₃ ⁻ and NH ₄ ⁺	Eppley and Peterson 1979
Neritic waters, estimated global annual average ^b	1,000	460	0.46	¹⁴ C uptake method	¹⁵ N-labeled NO ₃ ⁻ and NH ₄ ⁺	Eppley and Peterson 1979
Inshore waters, estimated global annual average ^b	340	102	0.30	¹⁴ C uptake method	¹⁵ N-labeled NO ₃ ⁻ and NH ₄ ⁺	Eppley and Peterson 1979
Central Long Island Sound, May–June 2010 ^c	719±538	182±37	0.25	Daytime net community production calculated from high-frequency ΔO ₂ in free water mass, corrected for air–sea gas exchange	Diel change in high-pass filtered [NO ₃ ⁻]	This study
Northern California coastal waters, 20 km west of Monterey Bay, average for station M1 of Johnson et al., 2004–2006	145±21 mgCm ³ day ⁻¹	99±11 mgCm ³ day ⁻¹	0.68±0.12	¹⁴ C uptake method	Diel change in high-pass filtered [NO ₃ ⁻]	Johnson et al. 2006
Apalachicola Bay, Florida, ecosystem average, 1994–1996	750±68 ^d	–	0.19 ^d	¹⁴ C uptake method	Extrapolated from net DIN input (Σ NH ₄ ⁺ , NO ₃ ⁻ , NO ₂ ⁻ , urea) based on ecosystem-level mass balance model	Mortazavi et al. 2000a, b
Carmans River estuary, Long Island, New York, annual average	–	–	0.37	¹⁴ C uptake method	¹⁵ N-labeled NO ₃ ⁻ , NH ₄ ⁺ , and urea	Carpenter and Dunham 1985

All values are reported in units of milligrams of C. Where necessary, to convert O₂-based measurements to units of C, we assumed a photosynthetic quotient of 1.2 (1.2 mol O₂:1 mol C). To convert parameters based on ΔNO₃⁻, we assumed Redfield stoichiometry (6.6 mol C/molN)

^a Reported as water column depth-integrated values of square meters per day⁻¹, except for values from the current study, which are reported as integrated measurements for the euphotic zone, and the estimates of Johnson et al. for northern California coastal waters, which are reported in volumetric units of per cubic meter per day

^b Estimates of annual productivity (square meter per year) were converted to estimated daily average rates by dividing by 365

^c Reported for only the portion of study period for which we had good nitrate data

^d Annual averages; peak GCP of 1,812 mgCm⁻² day⁻¹ was observed in summer; *f* ratio ranged from 0.11 in summer at low river flow to 0.74 in winter at peak DIN input

may explain why we did not consistently observe the expected response at our study site. In estuaries and other shallow waters, for example, the wind forcing that accompanies storm events can intensify turbidity and reduce available light even as mixed-layer deepening delivers nutrients

to the surface layer (Cloern 1987). This mechanism has been recently hypothesized in shallow systems where wind forcing penetrates into the sediment layer (Brand et al. 2010). Despite the central Sound's greater water depth and generally low turbidity, the data suggest wind-induced sediment

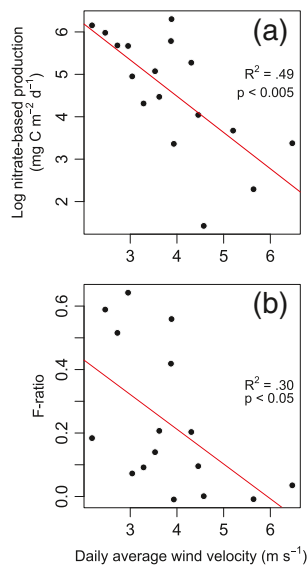


Fig. 9 Influence of wind velocity on **a** the daily NO_3^- based production rate and **b** daily estimates of the f -ratio at the Central Sound Buoy. Subset of data from May and June 2010

suspension might still have played some role in inhibiting photosynthetic uptake of newly delivered nitrate at our site.

Variations in Net Ecosystem Metabolism

While the differences between monthly mean rates of ecosystem metabolism were not significant, average values suggest the system transitioned from net autotrophy to trophic balance or net heterotrophy over the course of the study period. A June average of $585 \pm 389 \text{ mgCm}^{-2} \text{ day}^{-1}$ reflects a state of net autotrophy that dominated during the first half of the summer. By comparison, July and August means of 292 ± 235 and $494 \pm 456 \text{ mgCm}^{-2} \text{ day}^{-1}$, respectively, suggest the system trended toward even trophic status as sea surface temperatures at the site increased to nearly 25°C (Fig. 2e) and encouraged higher rates of respiration.

The transition to even trophic status or slight net heterotrophy reflected a steady decline in dissolved oxygen over the course of the study period (Fig. 2a). While this seasonal drawdown was not of the order of magnitude that accompanies the severe benthic hypoxia typical of westerly sites in the Sound (O'Donnell et al. 2008; Welsh and Eller 1991), it nevertheless reflects a unifying seasonal trend within the estuary.

The state of metabolic balance (or weak net autotrophy) we report for our study site suggests that the central Sound is more similar in many ways to the deeper, more evenly metabolically balanced coastal ecosystems that lie to its east than it is to the heavily eutrophic western Sound. Like many shallower temperate estuaries, western Long Island Sound is generally (and at times strongly) heterotrophic. In a study of

42 sites within 22 US estuaries, Caffrey (2004) found that just two systems—both of them in the northeastern USA—were net autotrophic in summertime. All 42 systems had average depths much shallower than that of Long Island Sound, and none of the sites had a depth approaching that of our study site. Waquoit Bay, a small estuary in Massachusetts, was significantly autotrophic in summer and exhibited weak net autotrophy throughout the year; the larger Narragansett Bay was markedly net heterotrophic in all seasons except winter (Table 3). Central Long Island sound appears in many ways similar to the lower, polyhaline reaches of the Chesapeake Bay, for which similar estimates of GPP ($1,670 \text{ mgCm}^{-2} \text{ day}^{-1}$), community respiration ($1,460 \text{ mgCm}^{-2} \text{ day}^{-1}$), and ecosystem metabolism ($210 \text{ mgCm}^{-2} \text{ day}^{-1}$) have been reported (Kemp et al. 1997). The shallower, more eutrophic upper reaches of the Bay were generally similar in trophic status to the western third of the Sound.

Challenges Inherent in Free-Water Mass Measurements of Ecosystem Metabolism

Dissolved Oxygen Anomalies

In this study, minimum rates of community respiration approached zero on eight separate dates, seven of which occurred at the outset of the study period in May. These were days on which we observed apparent nighttime increases in dissolved oxygen; because these anomalous nighttime increases would have yielded negative community respiration rates according to our method, we manually assigned to these days respiration rates of near zero. These dates encompassed some of the lowest temperatures observed during our study (a minimum daily average surface temperature of 12.9°C was noted on 22 May). While near-zero rates of community respiration are more commonly observed in winter months when Long Island Sound surface waters reach temperatures near freezing, near-zero rates have been previously observed in the Sound in May (Goebel and Kremer 2007).

Apparent nighttime production is evident on these dates even in the high-pass filtered dissolved oxygen dataset (Fig. 3c). On several days, two dissolved oxygen maxima are evident. The first is the expected, biologically driven midafternoon maximum that occurs on all study days, corresponding to both peak irradiance (Fig. 3d) and the daily nitrate minimum (red trace in Fig. 3c); the other dissolved oxygen maximum, however, occurs at nighttime, suggesting an abiotic process is responsible. Though unlikely, it is possible these instances of apparent dark oxygen production were the result of abiotic or biologically mediated hydrogen peroxide decomposition in surface waters during the night (Pamatmat 1997; Vermilyea et al. 2010).

However, concentrations of H_2O_2 typical of coastal waters in the northeastern USA (Moffett and Zafiriou 1990) would not support an O_2 input of the magnitude necessary to explain the increases we observed.

The magnitude of these nighttime anomalies (e.g., an apparent negative respiration rate of $-5,000 \text{ mg C m}^{-2} \text{ day}^{-1}$ on 22 May) suggests that we either overestimated evasion of O_2 to the atmosphere on these dates or that the hourly interval we used for our flux calculations was not sufficiently short to exclude variations in water mass properties caused by tidal advection. That seven of the eight instances occurred during the earliest phase of the study period strengthens our belief that the signal was masked on these dates by one or both of these physical processes. Water mass heterogeneity can be particularly confounding during periods of lower metabolic activity, when a weak biologically driven dissolved oxygen signal is easily overwhelmed by physical processes (Caffrey 2003; Swaney et al. 1999). The complex partitioning of variation in dissolved oxygen concentrations between physical and biological factors was noted in some of the earliest in situ estimates of ecosystem metabolism (Kemp and Boynton 1980).

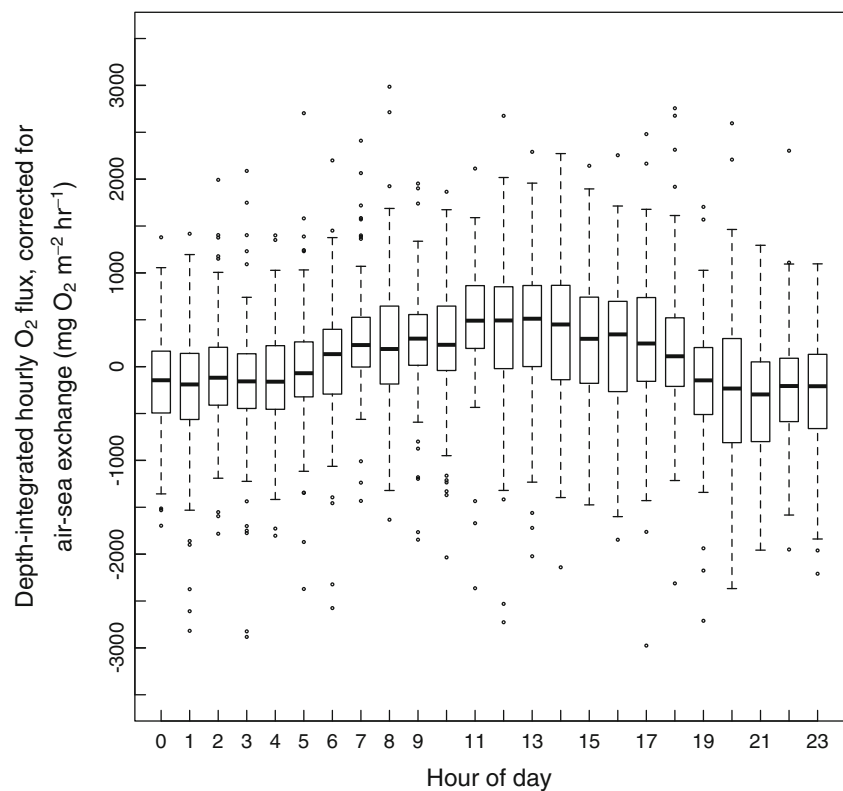
With the exception of these instances, hourly flux calculations ably captured the changing balance between photosynthetic oxygen production on the one hand and respiration (oxygen consumption) on the other (Fig. 10). The relative strength of these two opposing yet complementary processes yields the core biological signal typical of oxygen fluxes

in natural systems: Oxygen production rates rise steadily throughout the day to a peak in midafternoon as photosynthesis gradually outpaces oxygen consumption from respiration; as available light then decreases with the setting sun, respiration increasingly dominates. Net oxygen consumption is evident in the negative flux values that dominate evening and overnight hours.

While this common biological signal was evident in dissolved oxygen concentrations as they changed over the course of each individual study day, the many other physical and biological processes that regulate community metabolism in natural systems produced wide variations in hourly flux rates (see, e.g., the many individual flux measurements that lie outside the 5 and 95 % confidence intervals in Fig. 10).

Our methods allowed us to isolate biogeochemical processes from physical interferences to a very significant degree. However, as our results indicate, signal processing is not a panacea. One might alternatively have attempted to capture the impact of physical forcings, particularly the movement of different water masses, by deploying an array of multiple moorings over a relatively small spatial extent. This approach is not dissimilar to the many studies in rivers and other flowing waters (beginning with Odum 1956) that have attempted to follow the same water mass over its transit within a confined water body. Implementing this sort of experimental design at a site such as the one in this study would require significant investments in additional

Fig. 10 Box and whisker plot of the individual hourly oxygen hourly fluxes calculated during the study period ($n=1,896$), displayed by hour of day. During daylight hours, net oxygen production rises to a peak in midafternoon and then falls, in proportion to the amount of incident sunlight. During overnight hours, when only respiration takes place, net consumption of oxygen is evident. Fluxes were calculated according to Eq. 3. The upper and lower members of the boxes are the third and first quartiles of data in each category, respectively; whiskers roughly represent 5 and 95 % confidence intervals



instrumentation and field time; a simple, two-station, up-stream–downstream study design would not be adequate.

Air–Sea Exchange

The central Sound remained supersaturated with respect to dissolved oxygen throughout the study period, consistent with our overall finding of net autotrophy over the course of the study period. The magnitude of the air–sea flux varied significantly from day to day (see, e.g., Table 1), comprising, on average, 11 % of the total carbon flux. Both the degree of variability and the apparent magnitude of the flux relative to net ecosystem metabolism are consistent with estimates of air–sea exchange in other temperate estuaries (Caffrey 2004; D’Avanzo et al. 1996; Howarth et al. 1992; Kemp and Boynton 1980; Marino and Howarth 1993).

The fact that the air–sea flux accounts for so significant a percentage of the total organic matter processed with the ecosystem emphasizes the need for great care in selecting a model of air–sea gas exchange. A sensitivity analysis comparing the independent estimates based on each of the three gas exchange models to the mean values on which we based our analysis (Table 5) illustrates the significant impact assumptions about gas exchange can have on estimates of biogeochemical indicators. On a percentage change basis, our estimates of NEM were the most affected by modification of the gas exchange model. Our estimates of the f ratio also changed significantly under the various scenarios.

Conclusion

From continuous in situ measurements of dissolved oxygen and nitrate concentrations and several other ancillary biogeochemical parameters, we were able to discern significant hourly, daily, and seasonal variations in rates of GPP, new production, and NEM. While the balance between photosynthesis and respiration explained the majority of variation in nitrate concentration, wind stress modified the nitrate signal in ways both consistent and inconsistent with patterns of nitrate entrainment previously observed in the open ocean.

Coupled with measurements of primary production, estimates of new production and the f ratio may be used as diagnostic tools to evaluate the degree of eutrophication in estuaries over very short time scales, giving an oft-referenced and frequently re-examined model in chemical oceanography new utility. While its effectiveness as a measurement of the strength of the biological pump in the open ocean has been questioned (Yool et al. 2007), we suggest that the f ratio can be a valuable tool in near-coastal eutrophic ecosystems—provided one makes accurate assumptions about the nature and source of allochthonous nitrogen.

Because we derived our estimates almost exclusively from data gathered with in situ devices, we confronted significant challenges that accompany the many benefits of these new technologies. Investigators hoping to make the most of these instruments would do well to incorporate into the very earliest stages of study design robust schemes for validation and calibration of instrument data. Of equal

Table 5 Sensitivity analysis of air–sea gas exchange calculation, showing effect of chosen model on daily rates of GPP, R_c , and NEM and on the value of the f ratio

Metabolic parameter	Transfer velocity model	Daily mean value (mgCm ⁻² day ⁻¹ ±95 % CI)	Difference from 3-model mean (%)
GPP	3-model mean (basis for metabolic values reported in this study)	2,080±419	0
	Wanninkhof and McGillis (1999)	2,070±418	-0.48
	Raymond and Cole (2001)	2,100±419	+1.0
	Marino and Howarth (1993)	2,080±422	0
R_c	3-model mean	1,660±431	0
	Wanninkhof and McGillis (1999)	1,850±430	+11
	Raymond and Cole (2001)	1,540±430	-7.2
	Marino and Howarth (1993)	1,590±433	-4.2
NEM	3-model mean	426±203	0
	Wanninkhof and McGillis (1999)	219±201	-49
	Raymond and Cole (2001)	560±205	+31
	Marino and Howarth (1993)	498±205	+17
f ratio	3-model mean	0.25	0
	Wanninkhof and McGillis (1999)	0.32	+28
	Raymond and Cole (2001)	0.22	-12
	Marino and Howarth (1993)	0.24	-4.0

For GPP, R_c , and NEM, we evaluated the effect of model choice on the daily mean value for the entire study period (May–August). For the f ratio, we were able to evaluate only the effect on the May–June mean

necessity is the early and informed development of plans and contingencies to deal with biofouling, a vexing obstacle that continues to represent a major challenge in this exciting emerging field within the marine and aquatic sciences.

Acknowledgments We thank Mary Beth Decker, Elizabeth Hatton, David Butman, Charlie Munford, Lauren Brooks, Helmut Ernstberger, Jonas Karosas, Henry Wilson, Maura Bozeman, and Gabe Benoit for assistance with various aspects of research on Long Island Sound and sample analysis in New Haven. This work benefited from valuable discussions with Kung-Sik Chan, Michael Kemp, and members of the Van Mooy Lab at WHOI. Nicole Goebel and Roxanne Marino shared unpublished details of previous research. We are indebted to Ken Johnson for advice on calibration and operation of the SUNA and for some crucial MATLAB code. Lastly, we thank an anonymous reviewer for thoughtful criticism, which greatly improved our manuscript. The LISICOS network is supported by the National Oceanographic and Atmospheric Administration as part of the US Integrated Ocean Observing System. This work was supported by the Yale Institute for Biospheric Studies, the Sounds Conservancy of the Quebec-Labrador Foundation, and the Yale School of Forestry and Environmental Studies Carpenter-Sperry Fund.

References

- Andersen, V., and L. Prieur. 2000. One-month study in the open NW Mediterranean Sea (DYNAPROC experiment, May 1995): Overview of the hydrobiogeochemical structures and effects of wind events. *Deep Sea Research Part 1: Oceanographic Research Papers* 47(3): 397–422.
- Anderson, T.H., and G.T. Taylor. 2001. Nutrient pulses, plankton blooms, and seasonal hypoxia in western Long Island Sound. *Estuaries* 24(2): 228–243.
- Anisfeld, S.C., R.T. Barnes, M.A. Altabet, and T. Wu. 2007. Isotopic apportionment of atmospheric and sewage nitrogen sources in two Connecticut rivers. *Environmental Science & Technology* 41(18): 6363–6369.
- Antia, N.J., P.J. Harrison, and L. Oliveira. 1991. The role of dissolved organic nitrogen in phytoplankton nutrition, cell biology and ecology. *Phycologia* 30(1): 1–89.
- Arar, E.J., and G.B. Collins. 1997. *In vitro determination of chlorophyll a and phaeophytin a in marine and freshwater algae by fluorescence. Revision 1.2*. Cincinnati: U.S. Environmental Protection Agency, Office of Research and Development, National Exposure Research Laboratory.
- Balcilar, M. 2009. “mFilter” library for R: a language and environment for statistical computing. R Foundation for Statistical Computing, Vienna
- Bennett, D.C., J. O’Donnell, W.F. Bohlen, and A. Houk. 2010. Tides and overtimes in Long Island Sound. *Journal of Marine Research* 68(1): 1–35.
- Bigg, G.R., T.D. Jickells, A.H. Knap, and R. Sherriffidow. 1989. The significance of short-term wind induced mixing events for new primary production in subtropical gyres. *Oceanologica Acta* 12 (4): 437–442.
- Bowman, M.J. 1977. Nutrient distributions and transport in Long Island Sound. *Estuarine and Coastal Marine Science* 5(4): 531–548.
- Brand, A., J. R. Lacy, K. Hsu, D. Hoover, S. Gladding and M. T. Stacey. 2010. Wind-enhanced resuspension in the shallow waters of South San Francisco Bay: Mechanisms and potential implications for cohesive sediment transport. *Journal of Geophysical Research C: Oceans* 115(11)
- Breitburg, D.L., D.W. Hondorp, L.A. Davias, and R.J. Diaz. 2009. Hypoxia, nitrogen, and fisheries: Integrating effects across local and global landscapes. *Annual Review of Marine Science* 1: 329–349.
- Bronk, D.A., P.M. Gilbert, and B.B. Ward. 1994. Nitrogen uptake, dissolved organic nitrogen release, and new production. *Science* 265(5180): 1843–1846.
- Bushaw-Newton, K. L. and K. G. Sellner. 1999. *Harmful algal blooms. NOAA’s State of the Coast Report*. Silver Spring: National Oceanic and Atmospheric Administration. http://state-of-coast.noaa.gov/bulletins/html/hab_14/hab.html Accessed 16 December 2011.
- Caffrey, J. 2004. Factors controlling net ecosystem metabolism in U.S. estuaries. *Estuaries and Coasts* 27(1): 90–101.
- Caffrey, J.M. 2003. Production, respiration and net ecosystem metabolism in US estuaries. *Environmental Monitoring and Assessment* 81(1–3): 207–219.
- Capriulo, G.M., G. Smith, R. Troy, G.H. Wikfors, J. Pellet, and C. Yarish. 2002. The planktonic food web structure of a temperate zone estuary, and its alteration due to eutrophication. *Hydrobiologia* 475(1): 263–333.
- Carpenter, E.J., and S. Dunham. 1985. Nitrogenous nutrient uptake, primary production, and species composition of phytoplankton in the Carmans River estuary, Long Island, New York. *Limnology and Oceanography* 30(3): 513–526.
- Castro, M., C. Driscoll, T. Jordan, W. Reay, and W. Boynton. 2003. Sources of nitrogen to estuaries in the United States. *Estuaries and Coasts* 26(3): 803–814.
- Chan, K.-S. 2008. “TSA” library for R: a language and environment for statistical computing. Version 0.97. R Foundation for Statistical Computing, Vienna
- Chen, D., S.G. Horrigan, and D.P. Wang. 1988. The late summer vertical nutrient mixing in Long Island Sound. *Journal of Marine Research* 46(4): 753–770.
- Christensen, J.P., and H. Melling. 2009. Correcting nitrate profiles measured by the in situ ultraviolet spectrophotometer in Arctic Ocean waters. *The Open Oceanography Journal* 3: 59–66.
- Cloern, J.E. 1987. Turbidity as a control on phytoplankton biomass and productivity in estuaries. *Continental Shelf Research* 7(11–12): 1367–1381.
- Collos, Y. 1998. Nitrate uptake, nitrite release and uptake, and new production estimates. *Marine Ecology Progress Series* 171: 293–301.
- Cryer, J.D., and K.-S. Chan. 2008. *Time series analysis with applications in R*. New York: Springer.
- D’Avanzo, C., J.N. Kremer, and S.C. Wainright. 1996. Ecosystem production and respiration in response to eutrophication in shallow temperate estuaries. *Marine Ecology Progress Series* 141: 263–274.
- DeGrandpre, M.D., T.R. Hammar, D.W.R. Wallace, and C.D. Wirick. 1997. Simultaneous mooring-based measurements of seawater CO₂ and O₂ off Cape Hatteras, North Carolina. *Limnology and Oceanography* 42(1): 21–28.
- Diaz, R.J., and R. Rosenberg. 2008. Spreading dead zones and consequences for marine ecosystems. *Science* 321(5891): 926–929.
- Dugdale, R.C., and J.J. Goering. 1967. Uptake of new and regenerated forms of nitrogen in primary productivity. *Limnology and Oceanography* 12(2): 196–206.
- Eppley, R.W., and B.J. Peterson. 1979. Particulate organic matter flux and planktonic new production in the deep ocean. *Nature* 282 (5740): 677–680.
- Eppley, R.W., and E.H. Renger. 1988. Nanomolar increase in surface-layer nitrate concentration following a small wind event. *Deep Sea Research Part A. Oceanographic Research Papers* 35(7): 1119–1125.

- Garside, C. 1985. The vertical distribution of nitrate in open ocean surface water. *Deep Sea Research Part A. Oceanographic Research Papers* 32(6): 723–732.
- Goebel, N.L., and J.N. Kremer. 2007. Temporal and spatial variability of photosynthetic parameters and community respiration in Long Island Sound. *Marine Ecology Progress Series* 329: 23–42.
- Goebel, N.L., J.N. Kremer, and C.A. Edwards. 2006. Primary production in Long Island Sound. *Estuaries and Coasts* 29(2): 232–245.
- Hayduk, W., and H. Laudie. 1974. Prediction of diffusion coefficients for nonelectrolytes in dilute aqueous solutions. *AICHE Journal* 20(3): 611–615.
- Hopkinson, C.S., and E.M. Smith. 2005. Estuarine respiration: an overview of benthic, pelagic, and whole system respiration. In *Respiration in aquatic ecosystems*, ed. P. del Giorgio and P. Williams, 122–146. New York: Oxford University Press.
- Howarth, R.W., R. Marino, R. Garritt, and D. Sherman. 1992. Ecosystem respiration and organic-carbon processing in a large, tidally influenced river: The Hudson River. *Biogeochemistry* 16(2): 83–102.
- Hu, H.L., H.M. Chen, N.P. Nikolaidis, D.R. Miller, and X.S. Yang. 1998. Estimation of nutrient atmospheric deposition to Long Island Sound. *Water, Air, and Soil Pollution* 105(3–4): 521–538.
- Johnson, K.M., C.M. Burney, and J.M. Sieburth. 1981. Enigmatic marine ecosystem metabolism measured by direct diel sigma-CO₂ and O₂ flux in conjunction with DOC release and uptake. *Marine Biology* 65(1): 49–60.
- Johnson, K.S. 2010. Simultaneous measurements of nitrate, oxygen, and carbon dioxide on oceanographic moorings: Observing the Redfield ratio in real time. *Limnology and Oceanography* 55(2): 615–627.
- Johnson, K.S., and L.J. Coletti. 2002. In situ ultraviolet spectrophotometry for high resolution and long-term monitoring of nitrate, bromide and bisulfide in the ocean. *Deep Sea Research Part I: Oceanographic Research Papers* 49(7): 1291–1305.
- Johnson, K.S., L.J. Coletti, and F.P. Chavez. 2006. Diel nitrate cycles observed with in situ sensors predict monthly and annual new production. *Deep Sea Research Part I: Oceanographic Research Papers* 53(3): 561–573.
- Kemp, W.M., and W.R. Boynton. 1980. Influence of biological and physical processes on dissolved-oxygen dynamics in an estuarine system: Implications for measurement of community metabolism. *Estuarine and Coastal Marine Science* 11(4): 407–431.
- Kemp, W.M., E.M. Smith, M. MarvinDiPasquale, and W.R. Boynton. 1997. Organic carbon balance and net ecosystem metabolism in Chesapeake Bay. *Marine Ecology Progress Series* 150(1–3): 229–248.
- Kenefick, A.M. 1985. Barotropic M2 tides and tidal currents in Long Island Sound: A numerical model. *Journal of Coastal Research* 1(2): 117–128.
- Kirk, J.T.O. 1984. Attenuation of solar radiation in scattering-absorbing waters: A simplified procedure for its calculation. *Applied Optics* 23(21): 3737–3739.
- Kirk, J.T.O. 2003. The vertical attenuation of irradiance as a function of the optical properties of the water. *Limnology and Oceanography* 48(1): 9–17.
- Kirk, J.T.O. 2011. *Light and photosynthesis in aquatic ecosystems*. Cambridge: Cambridge University Press.
- Klein, P., and B. Coste. 1984. Effects of wind-stress variability on nutrient transport into the mixed layer. *Deep Sea Research Part A. Oceanographic Research Papers* 31(1): 21–37.
- Luo, Y., X. Yang, R.J. Carley, and C. Perkins. 2002. Atmospheric deposition of nitrogen along the Connecticut coastline of Long Island Sound: A decade of measurements. *Atmospheric Environment* 36(28): 4517–4528.
- Marino, R., and R. Howarth. 1993. Atmospheric oxygen exchange in the Hudson River: Dome measurements and comparison with other natural waters. *Estuaries and Coasts* 16(3): 433–445.
- Marra, J. 2009. Net and gross productivity: Weighing in with 14C. *Aquatic Microbial Ecology* 56(2–3): 123–131.
- Marra, J., R.R. Bidigare, and T.D. Dickey. 1990. Nutrients and mixing, chlorophyll and phytoplankton growth. *Deep Sea Research Part A. Oceanographic Research Papers* 37(1): 127–143.
- McCarthy, M., T. Pratum, J. Hedges, and R. Benner. 1997. Chemical composition of dissolved organic nitrogen in the ocean. *Nature* 390(6656): 150–154.
- Moffett, J.W., and O.C. Zafriou. 1990. An Investigation of hydrogen peroxide chemistry in surface waters of Vineyard Sound with H₂¹⁸O₂ and ¹⁸O₂. *Limnology and Oceanography* 35(6): 1221–1229.
- Mortazavi, B., R.L. Iverson, W. Huang, F.G. Lewis, and J.M. Caffrey. 2000a. Nitrogen budget of Apalachicola Bay, a bar-built estuary in the northeastern Gulf of Mexico. *Marine Ecology Progress Series* 195: 1–14.
- Mortazavi, B., R.L. Iverson, W.M. Landing, F.G. Lewis, and W.R. Huang. 2000b. Control of phytoplankton production and biomass in a river-dominated estuary: Apalachicola Bay, Florida, USA. *Marine Ecology Progress Series* 198: 19–31.
- Nixon, S. W. 1992. Quantifying the relationship between nitrogen input and the productivity of marine ecosystems. In *Proceedings of advanced marine technology conference (AMTEC)*, eds. M. Takahashi, K. Nakata and T. R. Parsons, 57–83. Tokyo, Japan.
- NYSDEC and CTDEP. 2000. A total maximum daily load analysis to achieve water quality standards for dissolved oxygen in Long Island Sound. *Prepared in conformance with Section 303(d) of the Clean Water Act and the Long Island Sound Study*. New York Department of Environmental Conservation and Connecticut Department of Environmental Protection, 73pp.
- O'Donnell, J., H.G. Dam, W.F. Bohlen, W. Fitzgerald, P.S. Gay, A.E. Houk, D.C. Cohen, and M.M. Howard-Strobel. 2008. Intermittent ventilation in the hypoxic zone of western Long Island Sound during the summer of 2004. *Journal of Geophysical Research: Oceans* 113(C9): C09025.
- Odum, H.T. 1956. Primary production in flowing waters. *Limnology and Oceanography* 1(2): 102–117.
- OSI. 2009. *Final report of total suspended sediment monitoring for New York waters. Power cable embedment operations*. New York: LIPA/CL&P Cable Replacement Project.
- Paerl, H.W. 1997. Coastal eutrophication and harmful algal blooms: Importance of atmospheric deposition and groundwater as “new” nitrogen and other nutrient sources. *Limnology and Oceanography* 42(5): 1154–1165.
- Paerl, H.W., and M.F. Piehler. 2007. Nitrogen and marine eutrophication. In *Nitrogen in the marine environment*, vol. 2, ed. D.G. Capone, M. Mulholland, and E. Carpenter, 529–567. Orlando: Academic.
- Pamatmat, M.M. 1997. Non-photosynthetic oxygen production and non-respiratory oxygen uptake in the dark: A theory of oxygen dynamics in plankton communities. *Marine Biology* 129(4): 735–746.
- Panofsky, H.A., and J.A. Dutton. 1984. *Atmospheric turbulence: Models and methods for engineering applications*. New York: Wiley.
- Pidcock, R., M. Srokosz, J. Allen, M. Hartman, S. Painter, M. Mowlem, D. Hydes, and A. Martin. 2010. A novel integration of an ultraviolet nitrate sensor on board a towed vehicle for mapping open-ocean submesoscale nitrate variability. *Journal of Atmospheric and Oceanic Technology* 27(8): 1410–1416.
- Probyn, T.A., H.N. Waldron, S. Searson, and N.J.P. Owens. 1996. Diel variability in nitrogenous nutrient uptake at photic and subphotic depths. *Journal of Plankton Research* 18(11): 2063–2079.
- Raymond, P.A., and J.J. Cole. 2001. Gas exchange in rivers and estuaries: Choosing a gas transfer velocity. *Estuaries* 24(2): 312–317.
- Redfield, A.C. 1934. On the proportions of organic derivatives in sea water and their relation to the composition of plankton. In *James Johnstone memorial volume*, ed. R.J. Daniel, 176–192. Liverpool: University Press of Liverpool.

- Riley, G.A. 1956. Oceanography of Long Island Sound, 1952–1954. III. Physical oceanography. *Bulletin of the Bingham Oceanographic Collection* 15: 15–46.
- Riley, G.A., and S.M. Conover. 1956. Oceanography of Long Island Sound, 1952–1954. III. Chemical oceanography. *Bulletin of the Bingham Oceanographic Collection* 15: 47–61.
- Ryther, J.H., and W.M. Dunstan. 1971. Nitrogen, phosphorus, and eutrophication in coastal marine environment. *Science* 171 (3975): 1008–1013.
- Sakamoto, C.M., K.S. Johnson, and L.J. Coletti. 2009. Improved algorithm for the computation of nitrate concentrations in seawater using an in situ ultraviolet spectrophotometer. *Limnology and Oceanography: Methods* 7: 132–143.
- Sharqawy, M.H., J.H. Lienhard, and S.M. Zubair. 2010. Thermophysical properties of seawater: A review of existing correlations and data. *Desalination and Water Treatment* 16(1–3): 354–380.
- Smith, V.H. 2007. Using primary productivity as an index of coastal eutrophication: The units of measurement matter. *Journal of Plankton Research* 29(1): 1–6.
- Staehr, P.A., J.M. Testa, W.M. Kemp, J.J. Cole, K. Sand-Jensen, and S.V. Smith. 2012. The metabolism of aquatic ecosystems: History, applications, and future challenges. *Aquatic Sciences* 74(1): 15–29.
- Swaney, D.P., R.W. Howarth, and T.J. Butler. 1999. A novel approach for estimating ecosystem production and respiration in estuaries: Application to the oligohaline and mesohaline Hudson River. *Limnology and Oceanography* 44(6): 1509–1521.
- Tedesco, M., W.F. Bohlen, M.M. Howard-Strobel, D.R. Cohen, and P.A. Tebeau. 2003. The MYSound Project: Building an estuary-wide monitoring network for Long Island Sound, U.S.A. *Environmental Monitoring and Assessment* 81(1): 35–42.
- Vermilyea, A.W., S.P. Hansard, and B.M. Voelker. 2010. Dark production of hydrogen peroxide in the Gulf of Alaska. *Limnology and Oceanography* 55(2): 580–588.
- Wanninkhof, R. 1992. Relationship between wind speed and gas exchange over the ocean. *Journal of Geophysical Research: Oceans* 97(C5): 7373–7382.
- Wanninkhof, R., and W.R. McGillis. 1999. A cubic relationship between air–sea CO₂ exchange and wind speed. *Geophysical Research Letters* 26(13): 1889–1892.
- Weiss, R.F. 1970. The solubility of nitrogen, oxygen and argon in water and seawater. *Deep Sea Research and Oceanographic Abstracts* 17(4): 721–735.
- Welsh, B.L., and F.C. Eller. 1991. Mechanisms controlling summertime oxygen depletion in western Long Island Sound. *Estuaries* 14(3): 265–278.
- Wu, Y., T. Platt, C.C.L. Tang, S. Sathyendranath, E. Devred, and S. Gu. 2008. A summer phytoplankton bloom triggered by high wind events in the Labrador Sea, July 2006. *Geophysical Research Letters* 35(10): L10606.
- Xu, J., R.R. Hood, and S.-Y. Chao. 2005. A simple empirical optical model for simulating light attenuation variability in a partially mixed estuary. *Estuaries* 28(4): 572–580.
- Yool, A., A.P. Martin, C. Fernandez, and D.R. Clark. 2007. The significance of nitrification for oceanic new production. *Nature* 447(7147): 999–1002.
- Zhang, J., D. Gilbert, A.J. Gooday, L. Levin, S.W.A. Naqvi, J.J. Middelburg, M. Scranton, W. Ekau, A. Pena, B. Dewitte, T. Oguz, P.M.S. Monteiro, E. Urban, N.N. Rabalais, V. Ittekkot, W.M. Kemp, O. Ulloa, R. Elmgren, E. Escobar-Briones, and A.K. Van der Plas. 2010. Natural and human-induced hypoxia and consequences for coastal areas: Synthesis and future development. *Biogeosciences* 7(5): 1443–1467.
- Zielinski, O., D. Voß, B. Saworski, B. Fiedler, and A. Körtzinger. 2011. Computation of nitrate concentrations in turbid coastal waters using an in situ ultraviolet spectrophotometer. *Journal of Sea Research* 65(4): 456–460.

Further Reading

- Connecticut Department of Energy and Environmental Protection (CTDEEP). unpublished data. Matt Lyman, Environmental Analyst, CTDEEP, 79 Elm Street, Hartford, Connecticut 06106–5127.